The Astrophysical Journal Letters, 885:L40 (31pp), 2019 November 10 https://doi.org/10.3847/2041-8213/ab4e9f

Organosulfur Compounds Formed by Sulfur Ion Bombardment of Astrophysical Ice Analogs: Implications for Moons, Comets, and Kuiper Belt Objects

Alexander Ruf[1], Alexis Bouquet[2], Philippe Boduch[3], Philippe Schmitt-Kopplin[4,5], Vassilissa Vinogradoff[1], Fabrice Duvernay[1], Riccardo Giovanni Urso[6], Rosario Brunetto[6], Louis Le Sergeant d'Hendecourt[1], Olivier Mousis[2], and Grégoire Danger[1]
[1] Université Aix-Marseille, CNRS, Laboratoire de Physique des Interactions Ioniques et Moléculaires (PIIM), Marseille, France; gregoire.danger@univ-amu.fr
[2] Aix Marseille Université, CNRS, CNES, LAM, Marseille, France
[3] Centre de Recherche sur les Ions, les Matériaux et la Photonique (CEA/CNRS/ENSICAEN/UCBN), CIMAP, CIRIL, GANIL, France
[4] Helmholtz Zentrum München, Analytical BioGeoChemistry, Neuherberg, Germany
[5] Technische Universität München, Chair of Analytical Food Chemistry, Freising-Weihenstephan, Germany
[6] Université d'Orsay, Institut d'Astrophysique Spatiale, CNRS, CNES, France
Received 2019 August 19; revised 2019 October 8; accepted 2019 October 16; published 2019 November 8

Abstract

Carbon, hydrogen, nitrogen, oxygen, and sulfur are the main elements involved in the solid-phase chemistry of various astrophysical environments. Among these elements, sulfur chemistry is probably the least well understood. We investigated whether sulfur ion bombardment within simple astrophysical ice analogs (originating from H_2O:CH_3OH:NH_3, 2:1:1) could trigger the formation of complex organosulfur molecules. Over 1100 organosulfur (CHNOS) molecular formulas (12% of all assigned signals) were detected in resulting refractory residues within a broad mass range (from 100 to 900 amu, atomic mass unit). This finding indicates a diverse, rich and active sulfur chemistry that could be relevant for Kuiper Belt objects (KBO) ices, triggered by high-energy ion implantation. The putative presence of organosulfur compounds within KBO ices or on other icy bodies might influence our view on the search of habitability and biosignatures.

Unified Astronomy Thesaurus concepts: Comets (280); Trans-Neptunian objects (1705); Classical Kuiper belt objects (250); Astrochemistry (75); Astrobiology (74); Experimental techniques (2078); Laboratory astrophysics (2004)

1. Introduction

Sulfur is of high interest in the context of (astro)chemical evolution and habitability. Several sulfur-bearing molecules have been observed in various astronomical environments. In the diffuse interstellar medium (ISM), various sulfur-bearing molecules, such as CS (Penzias et al. 1971), have been detected and the sulfur abundance has been observed to be close to the cosmic value (Sofia et al. 1994; Neufeld et al. 2015) whereas in dense molecular clouds, sulfur is found to be depleted (Prasad & Huntress 1982; Van Steenberg & Shull 1988; Jiménez-Escobar & Caro 2011; Vastel et al. 2018). A hypothesis suggested that the sulfur is locked in the form of OCS in icy grain mantles (Palumbo et al. 1997). A recent study has modeled that the "missing" sulfur is indeed trapped in the form of organosulfur molecules on grains (Laas & Caselli 2019). In protoplanetary disks, the planets' places of birth around young stars, CS or H_2CS chemistry has been discussed (Semenov et al. 2018; Le Gal et al. 2019). Nevertheless, the number of sulfur molecules detected in disks is significantly lower than in the diffuse ISM, indicating a high reactivity of sulfur in the gas phase (Semenov et al. 2018). In the solar system, comet 67P/Churyumov–Gerasimenko has been extensively characterized regarding its sulfur contents. C-, H-, and S-bearing molecules were found to be the third most abundant species, next to CH and CHO compounds (Altwegg et al. 2017). Among all sulfur compounds in comet 67P/Churyumov–Gerasimenko, even fairly complex organosulfur compounds have been detected (e.g., CH_3SH, methanethiol and C_2H_6S, ethanethiol, and/or dimethyl sulfide; Calmonte et al. 2016). On icy moons, as on the surface of Europa, the production of sulfuric acid and other sulfur compounds has been discussed (Carlson et al. 2002).

The reservoir(s) and evolution of organosulfur molecules, from the ISM toward their incorporation onto (proto)planetary systems, is poorly constrained. Radiation, as a ubiquitous source of energy in various astronomical environments, might be a potential trigger of organosulfur chemistry in space. For instance, energetic nuclei including sulfur are present in planetary radiation belts, solar wind or galactic and anomalous cosmic rays (GCR/ACR) (Mueller et al. 1991; Takashima et al. 1997; Von Steiger et al. 2000; Mauk et al. 2004; Paranicas et al. 2009). On Europa, the formation of H_2SO_4 has been supposed via radiolysis from energetic charged particle bombardment and is supported both by experiments (Strazzulla et al. 2007) and observations (Dalton et al. 2013). Next to the presented numerous observations of sulfur molecules in space, their chemistry, especially those of organosulfur, is not well understood yet (e.g., problem of sulfur depletion in dense clouds and star-forming regions but no sulfur depletion in diffuse clouds in the ISM; Calmonte et al. 2016; Le Gal et al. 2019).

Along with observations, laboratory experiments enable a better understanding of the chemical evolution of extraterrestrial ices (Herbst & Van Dishoeck 2009; Danger et al. 2013, 2016; Van Dishoeck 2014; Schlemmer et al. 2015; Öberg 2016; Fresneau et al. 2017). Sulfur chemistry in laboratory ice experiments has been mainly studied in two ways, (i) irradiation by nonsulfurous particles of sulfur-bearing ices (e.g., via UV photons (Chen et al. 2014), electrons (Maity & Kaiser 2013; Mahjoub et al. 2017; Poston et al. 2018)), or protons (Moore 1984; Moore et al. 2007; Ferrante et al. 2008; Strazzulla et al. 2009; Garozzo et al. 2010; Loeffler et al. 2011) and (ii) irradiation by S projectiles of non-sulfur-bearing ices (Strazzulla et al. 2007, 2009; Ding et al. 2013; Lv et al. 2013; Boduch et al. 2016). UV photons can induce the formation of more complex sulfur-bearing

molecules (OCS or CS_2) inside initial H_2S ices (Chen et al. 2014). Also, electrons can trigger the formation of complex S molecules (small sulfur allotropes or even complex organosulfur compounds within H_2S-bearing ices) (Mahjoub et al. 2017). Protons enable the formation of OCS out of initially bearing SO_2 or H_2S ices as well (Ferrante et al. 2008; Garozzo et al. 2010). The implantation of S ions inside pure water ices leads to the production of sulfuric acid (Strazzulla et al. 2007; Ding et al. 2013). Inside CO and CO_2 ices, the bombardment of sulfur ions initiate the formation of SO_2 (Lv et al. 2013). Furthermore, molecular dynamics simulations suggest the formation of complex organosulfur molecules via S ion bombardment of H_2O:CO:NH_3:CH_3OH ices (Anders & Urbassek 2018, 2019). However, the formation of complex organosulfur molecules has never been experimentally demonstrated up to now.

In this study, the role of sulfur implantation into astrophysically relevant, realistic ice analogs (de Marcellus et al. 2015; Meinert et al. 2016) was tested. The resulting refractory residue was probed for the formation of organosulfur compounds via infrared spectroscopy (IR) and ultra-high-resolving electrospray ionization Fourier transform resonance cyclotron mass spectrometry (FT-ICR-MS). The sulfur-irradiated sample (S^{7+} ions) was compared to a reference sample which was processed with Argon (Ar^{7+} ions). FT-ICR-MS analyses enabled the first detection of organosulfur compounds within H_2O:CH_3OH:NH_3 ices (2:1:1), implanted with sulfur ions. Their detection and chemical characterization is discussed in the context of S^{7+}-irradiated ices of various astrophysical environments, particularly focusing on Kuiper Belt objects (KBO).

2. Methods

2.1. Formation of Ion-irradiated Ice Residue and IR In Situ Analysis

The ion beam used for irradiation was generated at the ARIBE low-energy line of the Grand Accélérateur National d'Ions Lourds (GANIL), Large Heavy Ion National Accelerator, facilities in Caen, France. For both Ar^{7+} and S^{7+}, the ion beam was formed by ions at an energy of 105 keV, with a flux of $\approx 1 \times 10^{11}$ cm^{-2} s^{-1}. The current reaching the vacuum chamber was controlled by a Faraday cup. The main vacuum chamber contained three windows out of ZnSe that can be cooled down to 9 K and could hold one sample each. Ice samples were formed by preparing a gas mixture in a premixing chamber and depositing this vapor using a mobile needle, allowing target deposition onto a desired window. This device effectively enabled the generation and irradiation of three different deposited samples at similar vacuum conditions. Details on beam generation (Lv et al. 2012) and the IGLIAS device (Augé et al. 2018) have been described previously.

The IGLIAS setup also enabled in situ chemical analysis of the sample by a Brüker V70 Fourier Transform Infrared Spectrometer (FT-IR), under primary vacuum while it is exposed to the beam. IR spectra were acquired before deposition (as a reference background), during irradiation (one spectrum after a new layer was deposited and before it was exposed to the beam, Figure 5) and after warming up to room temperature (one spectrum of the residue at 300 K, Appendix A). A residue is defined here as the refractory remaining material from irradiated ices at 300 K.

Ices were formed with an initial gas mixture of H_2O:CH_3OH:NH_3 (2:1:1). The quantity deposited corresponds roughly to 0.5 μm which is thicker than the penetration depths of 105 keV S^{7+} or Ar^{7+}, calculated to be <0.3 μm (Ziegler et al. 2010). Thus, implantation of projectile ions into the ice could be ensured. The windows were kept at 10 K during deposition and irradiation. To increase the yield of formed residue, we deposited several layers of each sample. A new layer is deposited when the underneath irradiated layer reaches a steady state. The evolution during the irradiation is monitored by FT-IR spectroscopy on both methanol and ammonia infrared absorption bands. This procedure was repeated. In total, 15 layers were formed for the argon-irradiated sample (Ar^{7+} ions) and 10 layers for the sulfur-irradiated sample (S^{7+} ions). The experiment was repeated (technical duplicates) later generating two 15-layer samples to test for reproducibility (for both Ar^{7+}-irradiated and S^{7+}-irradiated). Both duplicates show reproducible results.

We performed SRIM simulations (SRIM, The Stopping and Range of Ions in Matter software; Ziegler et al. 2010) to calculate the effective volume of atom implantation. We assume a sample density of 1 g/cm^{-3}. We find that sulfur ions stop on average at a depth of 0.21 ± 0.1 μm within the sample (2σ interval). Within the implanted volume, we estimate the signal-to-noise ratio (S/N) and S/C ratio to be 9E-4 at the end of the irradiation experiments (after 20 minutes). Even accounting for uncertainties on SRIM simulations and the sample density probably being below 1 g/cm^{-3}, it is readily apparent that the amount of implanted sulfur is small compared to the elements it can react with.

We have calculated that the irradiated volume (from the surface of the sample to a depth of 0.31 μm) receives a dose of 65 MGy (about 11 eV/16 amu).

The residues, resulting from irradiated ices, were kept under argon atmosphere in a stainless steel vessel, to minimize oxidation prior to analysis (de Marcellus et al. 2015).

2.2. FT-ICR-MS Analysis

Electrospray ionization Fourier transform ion cyclotron resonance mass spectrometry (FT-ICR-MS), ran in negative ionization mode, was used for in-depth molecular characterization of the organic matter formed within the residue, resulted from irradiated ices. High resolution mass spectrometry has been widely used for in-depth molecular characterization of extraterrestrial organic matter (Schmitt-Kopplin et al. 2010; Ruf et al. 2017, 2018, 2019; Danger et al. 2016; Fresneau et al. 2017). FT-ICR-MS represents the highest performance in mass resolving power and mass precision among all mass spectrometers.

The residue was dissolved in 50 μL methanol (extraction solvent, LC-MS grade; Fluka). This step was repeated four times. The complete residue got dissolved in methanol. Afterwards, 20 μL of the dissolved residue was diluted in 200 μL methanol. The solution was removed with a microsyringe, ready for flow injection into the ESI source. A solvent methanolic blank was measured in accordance to be able to detect the indigenous soluble organic matter in each ice sample.

The experimental study was performed on a high-field FT-ICR-MS from Bruker Daltonics with a 12-T magnet from Magnex. A time domain transient with four MWords was obtained and Fourier-transformed into a frequency domain spectrum. The frequency domain was afterward converted to a mass spectrum by the solariX control program of Bruker Daltonics. The ion excitations were generated in broadband mode (frequency sweep radial ion excitation) and 3000 scans were accumulated for each mass spectrum in a mass range of

147 to 1000 amu (atomic mass unit). Ions were accumulated for 300 ms before ICR ion detection. The pressure in the quadrupole/hexapole and ICR vacuum chamber was 3×10^{-6} mbar and 6×10^{-10} mbar, respectively. For CID-MS/MS, ions were accumulated for 3 s.

The electrospray ionization source (ESI, Apollo II; Bruker Daltonics) was operated in negative ionization mode. The methanolic solutions were injected directly into the ionization source by means of a microliter pump at a flow rate of 120 μL h^{-1}. A source heating temperature of 200°C was maintained and no nozzle-skimmer fragmentation was performed in the ionization source. The instrument was previously externally calibrated by using arginine negative cluster ions (5 mg L^{-1} arginine in methanol).

Mass spectra with *m/z* from 147 to 1000 amu were calibrated externally and internally to preclude alignment errors. Subsequently, mass spectra were exported to peak lists at a signal-to-noise ratio $\geqslant$3. Mass resolving power was 400,000 at $m/z = 400$ with a mass accuracy of $<$200 ppb, enabling the separate detection of isobars differing by less than the mass of an electron (Ruf et al. 2017). Practically, this approach enables a direct assignment of molecular compositions with C, H, N, O, and S atoms (and isotopologues in natural abundance) for each individual exact mass (m/z value).

Molecular formulas were assigned from exact m/z values by mass difference network analysis for each peak in batch mode by an in-house software tool (Tziotis et al. 2011) and validated via the senior-rule approach/cyclomatic number (Senior 1951). For formula assignment, 50.1% of all formulas have an error of $\pm$0.1 ppm, 78.5% of all formulas have an error of $\pm$0.2 ppm and 100% of formula assignments within $\pm$0.5 ppm (Figure 8). Further details on the assignment of molecular formulas from FT-ICR-MS big data and their visualization in astrochemical context are given in previous studies (Schmitt-Kopplin et al. 2010; Ruf et al. 2018; Bischoff et al. 2019).

Data mining on organosulfur (CHNOS) compounds represent those m/z signals which were uniquely detected in the S^{7+}-irradiated sample and absent in the Ar^{7+}-irradiated sample. Double bond equivalent (DBE) was calculated according $DBE = C - (H/2) + (N/2) + 1$.

3. Results and Discussion

3.1. Detection of Organosulfur Compounds

IR spectra of S^{7+}- and Ar^{7+}-irradiated ices and residues show the presence of organic compounds which have also been previously observed in UV-irradiated ices (e.g., HNCO or H_2CO; Figure 5, Table 1). Nevertheless, no significant difference between both irradiation sources, S^{7+} and Ar^{7+}, could be deciphered with infrared spectroscopy, and neither organosulfur molecules could be identified in the S^{7+}-irradiated sample.

On a coarse level, mass spectra from FT-ICR-MS analysis show similar features for Ar^{7+}-irradiated and S^{7+}-irradiated ices as well (Figures 1(A) and (B)). Nevertheless, the fine structure obtained with ultrahigh resolving power and ultrahigh mass accuracy, FT-ICR-MS unambiguously revealed the detection of organosulfur compounds in S^{7+}-irradiated ices (Figures 1(C) and (D)). m/z signals which correspond to organosulfur compounds were absent in the Ar^{7+}-irradiated reference sample (Figures 1(C) and (D)). Within one nominal mass, up to five organosulfur (CHNOS) signals are present as shown for two representative examples ($m/z = 248$ and $m/z = 438$, Figures 1(C) and (D)).

In general, the mass spectra of S^{7+}- and Ar^{7+}-irradiated refractory residues show dense m/z signal patterns over a broad mass range. From 30,000 experimental m/z signals, ranging from 100 to 900 amu (atomic mass unit), 9,616 molecular formulas, based on C, H, N, O, and S, could be unequivocally calculated (5.3% CHO, 82.6% CHNO, and 12.1% CHNOS, Figures 9 and 10). This high molecular diversity indicates a rich and active sulfur chemistry within these processed ices, triggered by high-energy ion implantation. m/z signals appear as regular patterns reflecting a pure chemosynthetic process as observed in UV photon-irradiated ices (Danger et al. 2013, 2016; Fresneau et al. 2017) or meteorites (Schmitt-Kopplin et al. 2010; Ruf et al. 2017, 2019; Figures 1(A) and (B)). Regular patterns are observed both for the global organic signature and for organosulfur (CHNOS) compounds (Figures 1(A) and (B)).

3.2. Characterization of Organosulfur Compounds

Atomic ratio plots, known as van Krevelen diagram (Van Krevelen 1950), were used to characterize in detail the detected organosulfur (CHNOS) compounds. H/C against O/C representation enables a first screening of complex mixtures with respect to chemical families (Kim et al. 2003; Wu et al. 2004; Danger et al. 2016; Ruf et al. 2018; Schmitt-Kopplin et al. 2019). Organosulfur compounds present in S^{7+}-irradiated ices show a low degree of unsaturation and a significant degree of oxygenation ($O/C > 0.5$, $H/C > 1.5$, Figure 2). The degree of oxygenation of organosulfur compounds is inversely related with DBE (Figures 2 and 12).

Basically, three groups of compounds can be extracted (Figure 2). Group 1 (Figure 2, top right corner) basically consists of small mass molecules up to 400 amu. This group of compounds has high H/C and high O/C ratios with a small number of DBE. Group 2 (Figure 2, top left corner) bears molecules with high masses (mostly 500–800 amu). Their DBE is higher than those in group 1 ($DBE > 8$, Figure 12). In addition, this group of compounds is enriched in nitrogen counts, bearing up to 14 N atoms per molecular formula (Figure 11). Group 3 (Figure 2, bottom left corner) is characterized by high numbers of DBE within a mass range between 400 and 600 amu (Figures 2 and 12).

A large number of identified organosulfur compounds are saturated molecules, having an averaged DBE of 5.6 (Figure 3). Nevertheless, DBEs of up to 17 are observed, especially for high-mass molecules up to 900 amu (Figure 3 and 10). Compounds with high DBE have low H/C and low O/C ratios (Figure 12).

The number of atoms for every element varies for the identified organosulfur compounds (Figures 4 and 13). Almost all organosulfur (CHNOS) compounds bear one sulfur atom and only a few molecular formulas have up to five S atoms. The aforementioned high degree of oxygenation is directly related to the number of oxygen atoms. Most CHNOS formulas possess eight O atoms. This might be related to the partially oxidized carbon starting material (CH_3OH, $O/C = 1$). This enables the formation of a complex organic molecules with a oxygen-rich carbon backbone (Theulé et al. 2013). These findings are in agreement with results from UV-irradiated ices (Danger et al. 2016). Nitrogen counts are also widespread, ranging mostly from 3 to 10 N atoms per CHNOS molecular formula. The carbon backbone counts indicate two local maxima in stability in C counts, for $C = 9$ and $C = 25$. Overall, the diversity in CHNOS formulas is related to a

Table 1
Spectral Features and their Attribution for the Ices Post-irradiation (Figure 5)

Position (cm^{-1})	Assignment	Species	Source
2340	$\nu_{as}(CO_2)$	**CO_2**	(Gerakines et al. 1994)
2275	ν(NCO)/ ?	$HOCN/CO_2$	(Schutte et al. 1993; Signorell et al. 2006)
2169	ν(NCO)	**OCN^-**	(Hudson et al. 2001; Raunier et al. 2003)
2140		**CO**	(Gerakines et al. 1996)
2089	ν(CN)and/or $\nu(^{13}CO)$	HCN and/or CO	(Maki & Blaine 1964)
1750-1700	ν(C=O)	H_2CO and other aldehydes	(Bisschop et al. 2007)/(Bossa et al. 2009)
1723	ν(C=O)	H_2CO	(Schutte et al. 1993)
1689	ν(C=O)	$HCOOH/NH_2COOH$?	(Bisschop et al. 2007)/(Bossa et al. 2009)
1585	ν(CO-O)	$HCOO^-$	(Schutte et al. 1999) and ref. therein
1494	δ(CH)	H_2CO	(Schutte et al. 1993)
1478		NH_4^+	(Schutte et al. 1999) and ref. therein
1461		NH_4^+	(Schutte et al. 1999) and ref. therein
1387	δ(CH)	$HCOO^-/HCOOH$	(Schutte et al. 1999) and ref. therein
1353	ν(CO-O)	$HCOO^-$	(Schutte et al. 1999) and ref. therein
1304		CH_4	(Kerkhof et al. 1999)
660		CO_2	(Colthup 1950)

Note. We only discuss here features that differ from the pre-irradiation spectrum (Figure 5, black label). All species assignments are tentative except the ones in bold.

diversity in atom counts therein. The observed large diversity in atom counts indicates a rich and active sulfur chemistry.

On average, a stoichiometric formula of $C_{13}H_{23}O_7N_6S$ is calculated, having a DBE (average) = 5.6, O/C (average) = 0.6 and H/C (average) = 1.8.

As observed from UV-irradiated ices (Danger et al. 2016), Ar^{7+}-irradiated and S^{7+}-irradiated ices (Figure 9), CHNO represents the major chemical family. This implies that pathways for CHNO formation in all cases are likely based on radical chemistry (Theulé et al. 2013; Butscher et al. 2017). Among the organosulfur (CHNOS) compounds observed in S^{7+}-irradiated residues, almost all of them bear only one sulfur atom (Figures 4, 10, and 13) and all organosulfur species bear nitrogen atoms (only CHNOS and no CHOS compounds got detected, Figure 9). These findings indicate a selective mechanism of organosulfur formation that is not well understood yet. The irradiating agent, S^{7+} or Ar^{7+}, might act chemically inert in a first step (similarly as UV photons), by breaking bonds and triggering radical and ion formation leading to precursor of complex CHNO compounds. Then CHNO precursors might selectively react with sulfur implemented in the water matrix forming $CHNOS_1$ species. The low number of S in organosulfur compounds can be explained by low S/N and S/C ratios (9E-4) in the implantation zone (see "SRIM simulations," Methods Section 2.1). Thus, the likelihood of implanting a sulfur atom into more complex organic molecules is low. The test of this hypothesis is beyond this manuscript and is part of ongoing work.

3.3. Astrophysical Implications

Several astrophysical environments reflect parallels with the here presented experiments.

The icy surface of the Jovian satellite Europa is exposed to a bombardment of energetic electrons and ions, including sulfur (Paranicas et al. 2009). This flux is abundant in the 100 keV range which was used in the experiments presented here. A calculation, based on flux (Paranicas et al. 2009), shows that 20 to 30 minutes of exposure to the sulfur beam in the IGLIAS chamber correspond to a few days on Europa's surface in terms of fluence. However, neither methanol nor ammonia have been detected on Europa (Carlson et al. 2009) and the surface temperature of 80–130 K (Spencer et al. 1999) is noticeably higher than the temperature at which irradiation was performed in our experiments. Nevertheless, the parallel with Enceladus allows us to consider the putative presence of both ammonia and methanol within Europa's internal ocean (Hodyss et al. 2009; Waite et al. 2017); and micrometeoroid bombardment represents a possible source of organic matter being transported to its surface (Carlson et al. 2009). However, as CO_2 represents the dominant form of carbon and the presence of NH_3 is uncertain, one should be cautious about direct implications of the results discussed here to Europa.

Further from the Sun, trans-Neptunian objects (TNOs) and KBOs present surface temperatures closer to our experimental conditions (e.g., 44 K on Orcus: Barucci et al. 2008). Ammonia has been detected on several of these objects, e.g., on Charon (Brown & Calvin 2000; Grundy et al. 2016), on Orcus (Barucci et al. 2008), or on Quaoar (Jewitt & Luu 2004). Both ammonia and methanol are present in comets (Bockelée-Morvan et al. 2004; Altwegg et al. 2017) suggesting their presence in the material that has formed TNOs/KBOs. These objects are exposed to irradiation by solar wind including small quantities of sulfur at about 32 keV/nucleus (derived from the solar wind velocity; Von Steiger et al. 2000), an energy comparable to the one used in the experiments presented here. Using the S/O ratios measured in the solar wind at 1 au (von Steiger et al. 2010) and extrapolating to the flux at 50 au, the fluence used in our experiments is approximated to be reached in 2 Myr. This relatively short time (on astronomical timescales) indicates that icy surfaces of objects such as TNOs/KBOs, possibly rich in ammonia and methanol, may have endured the same transformation as our laboratory samples. Interestingly, 2 Myr is shorter than the predicted time of destruction of ammonia hydrates by solar wind (Cooper et al. 2004; Jewitt & Luu 2004). Thus, NH_3 might still be stable enough to be further processed by sulfur ion bombardment to putatively form organosulfur compounds. This time is short enough that the building blocks of these bodies (e.g., small grains, ice) may interact with sulfur ions from solar wind before their accretion (assuming a similar composition of the solar wind at that time).

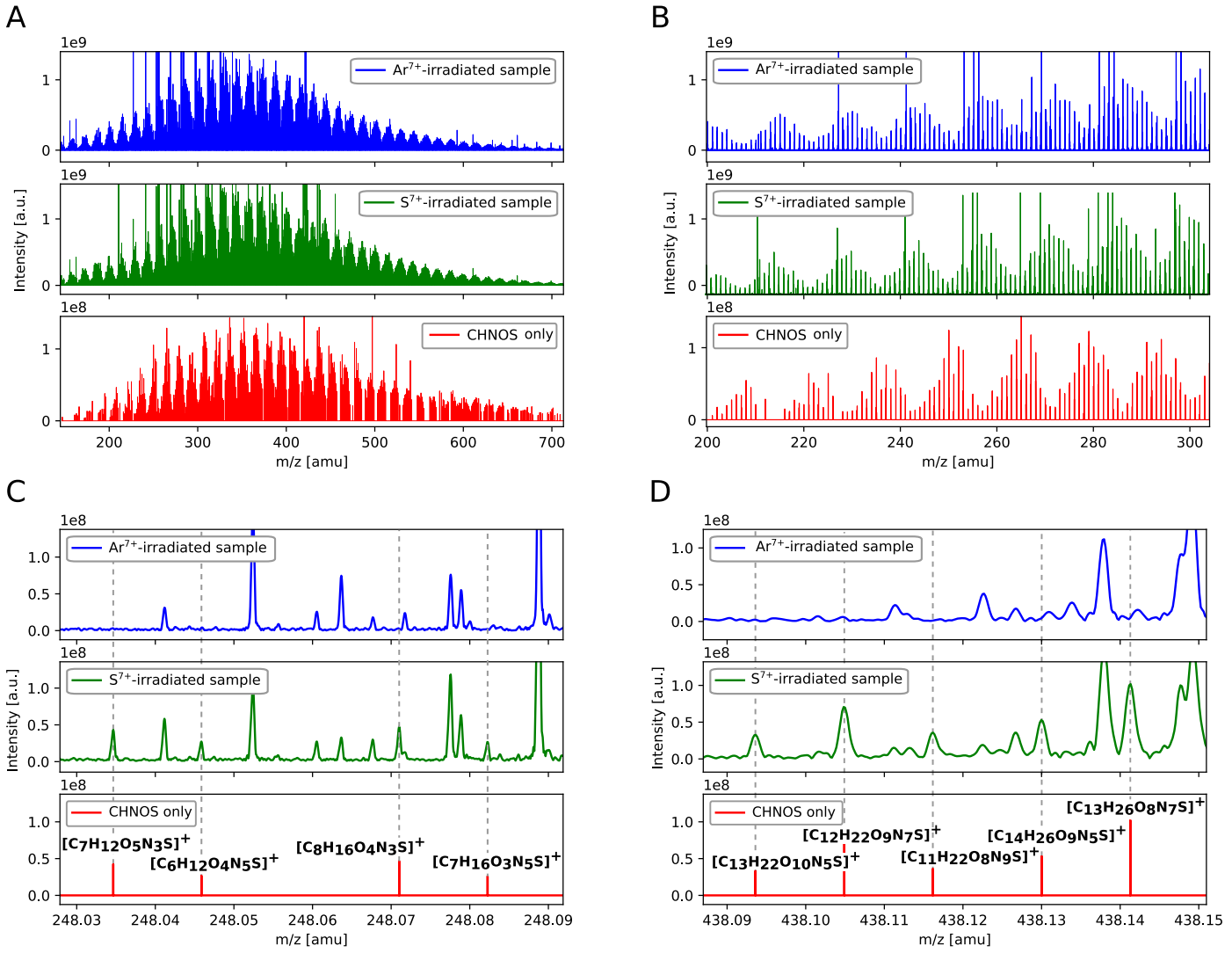

Figure 1. FT-ICR-MS revealed the detection of organosulfur compounds. (A) Mass spectra show a large number of m/z signals over broad mass range, from 150 to 700 amu (atomic mass unit), for both the Ar^{7+}- and S^{7+}-irradiated ice sample. Over 1100 unique organosulfur signals (CHNOS) are distributed over that mass range as well (Figure 10, Table 3). The "CHNOS only" spectrum has been reconstructed from experimental data (only CHNOS-corresponding m/z values are plotted). Organosulfur signals were absent in the Ar reference spectrum. (B) A zoomed-in representation shows repetition of signal patterns. (C, D) Detailed nominal mass spectra of $m/z = 248$ and $m/z = 438$ highlight the need for ultra-high-mass resolution and ultra-high-mass accuracy to enable the unambiguous differentiation of CHNOS molecular formulas in the S^{7+}-irradiated sample from non-sulfur-bearing ones in the Ar^{7+}-irradiated sample.

This is likely applicable to comets as well. The D/H ratio of comet 67P, for example, indicates a formation at a large distance from the Sun (Altwegg et al. 2015). So, ion implantation would have occurred at low temperatures. It should be noted that due to their formation beyond the H_2S snowline, the aforementioned objects (TNOs/KBOs) are likely to include H_2S, another putative source of sulfur chemistry. The presence of H_2S is supported by comparisons between laboratory experiments and IR spectra of KBOs and Trojan asteroids (Poston et al. 2018).

It is critical to note that thermal processing might be a factor driving the formation of complex organosulfur compounds. The surfaces of a KBO or TNO is unlikely to have undergone such processes. However, some of these objects could later get closer to the Sun and lose the more volatile components of their external layers, as has been suggested for Ceres (De Sanctis et al. 2015), undergoing a more modest thermal processing than in our experiments. On the other hand, we may also consider thermal processing of the interior of these objects, combined with the possibility that most of the ice, not only on the surface, has been implanted with sulfur before the object accreted. Accretional heat and radiogenic heating could have provided thermal processing to relatively high temperatures, especially in the larger objects such as Pluto, Charon, or Triton. In the case of Triton tidal heating may also have been a contributor (Ross & Schubert 1990). Contemporary cryovolcanic activity (Jewitt & Luu 2004; Cook et al. 2007; Desch et al. 2009) could then bring possible organosulfur molecules to the surface. Future missions to KBO/TNOs, comets, or even Neptune (if observations of Triton are included) could uncover these compounds.

4. Conclusions

The formation of complex organosulfur molecules by sulfur ion bombardment within simple, realistic ice analogs was tested. H_2O, CH_3OH, and NH_3 ices (2:1:1) were irradiated with S^{7+} ions at 105 keV at GANIL, Large Heavy Ion National Accelerator facilities in Caen, France. Sulfur-irradiated samples

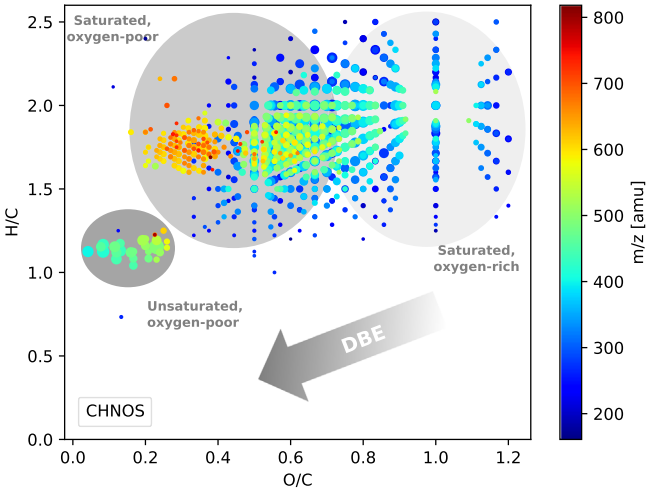

Figure 2. van Krevelen diagram (H/C against O/C) of organosulfur (CHNOS) compounds reveals information on different chemical families. Chemical compositions can be grouped according to the degree of unsaturation and relative oxygen amounts. The plotted CHNOS data correspond to m/z signals which are uniquely present in the S^{7+}-irradiated ice but not in the Ar^{7+}-irradiated ice sample. The bubble size scales with mass spectrometric intensity.

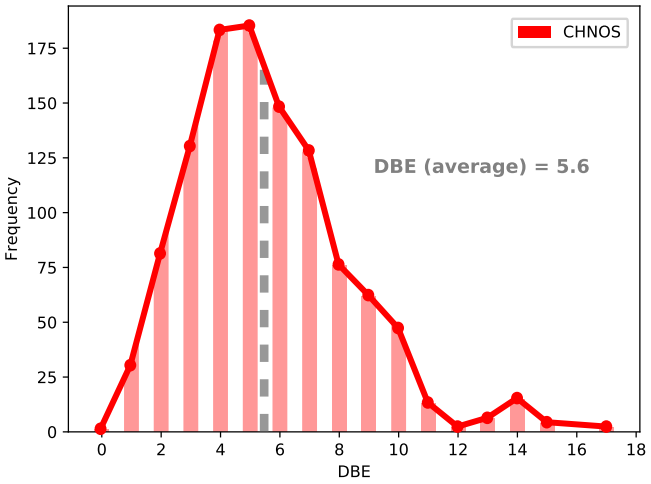

Figure 3. Frequency distribution of organosulfur (CHNOS) compounds as a function of DBE, double bond equivalent. The detected organosulfur compounds have an averaged DBE of 5.6, representing a significant amount of saturated molecules.

(S^{7+} ions) were compared to a reference sample which was processed similarly with argon (Ar^{7+} ions). Residues formed from ice processing were then analyzed by ultra-high-resolution mass spectrometry (FT-ICR-MS).

We unambiguously detected organosulfur compounds within sulfur-bombarded ices. Over 1100 organosulfur (CHNOS) molecular formulas (12% of all assigned signals) were observed within a broad mass range, from 100 to 900 amu (Figure 10, Table 3). On average, a stoechiometric formula of $C_{13}H_{23}O_7N_6S$ is calculated, having an DBE (average) = 5.6, O/C (average) = 0.6 and H/C (average) = 1.8.

There are multiple instances in the outer solar system in which water ice with methanol and ammonia could be undergoing or have undergone sulfur implantation. These include icy moons, KBOs/TNOs/comets, and their original building blocks. The experiments presented here indicate that with later thermal processing, these objects could feature a large diversity of complex organosulfur molecules such as the ones detected in the present work. These compounds could have participated in prebiotic chemistry and could be accessible to detection by future space missions performing in situ measurements.

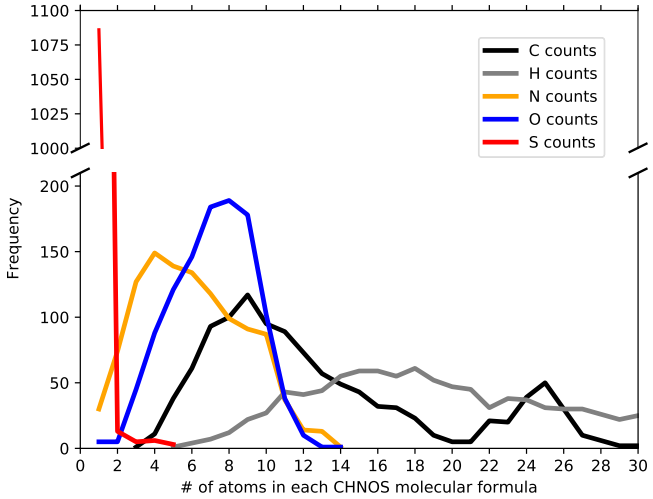

Figure 4. Frequency distribution of the number of molecular formulas as a function of the corresponding number of C, H, N, O, and S atoms in a CHNOS molecular formula. The observed large diversity in atom counts indicates a rich and active sulfur chemistry.

This work has been funded by CNRS (Programme National de Planétologie, P.N.P, INSU), Programme de Physique et Chimie du Milieu Interstellaire (PCMI, INSU), and the Centre National d'Etudes Spatiales (CNES, exobiology program). It was also supported by the French Agence Nationale de la Recherche (VAHIIA grant ANR-12-JS08-0001 and RAHIA SSOM grant ANR-16-CE29-0015) and from the Excellence Initiative of Aix-Marseille University—A*MIDEX, a French "Investissements d'Avenir programme."

Appendix A
IR Spectra

Supplementary figures and tables regarding the IR analysis. In the following, details on IR analysis are given. Spectra of both ices at 10 K (Figure 5, Table 1, Figure 6) and of residues at 300 K (Figure 7, Table 2) are shown.

IR spectrum of ices at 10 K (before and after irradiation). A comparison between the spectra of the samples at 10 K after irradiation (Figure 5) shows no significant difference in the features present between the argon-irradiated sample (Ar^{7+} ions) and the sulfur-irradiated sample (S^{7+} ions). In addition to the expected features of remaining water, methanol and ammonia, the spectra show carbon monoxide and dioxide, formaldehyde, and ammonium ions. Some other features are attributable to nitrogenated molecules or ions such as HCN or OCN^-. These products are consistent with previous experiments on these type of ices.

IR spectrum of the residues at 300 K (after irradiation). A comparison between the spectra of the samples at 300 K (refractory residues) is given in Figure 7. Both spectra show similar IR features, assigned to formiate or methanoate ions and to chemical functions such as amides, carboxylic acids, imines, and alcanes, consistent with previous studies (Table 2). Of note, in the sulfur-irradiated sample (S^{7+} ions), the presence of CO_2 and OCN^- features, more pronounced than in the argon-irradiated sample (argon-irradiated sample; Ar^{7+} ions), indicates

Table 2
Spectral Features and Their Attribution for the Residue at 300 K (Figure 7)

Position (cm^{-1})	Assignment	Species	Source	Difference between Spectras?
2338	ν(CO)	**CO_2**	(Gerakines et al. 1996)	More pronounced in S-irr
2214		Alkynes?	(Colthup 1950)	
2160	ν(NCO)	**OCN^-**	(Raunier et al. 2003)	More pronounced in S-irr
1726		Carboxylic acids/aldehydes/imines	(Colthup 1950)	
1669	ν(C=O)	Amides/carbamic acid	(Muñoz Caro & Schutte 2003)	
1589	ν(COO^-)	$HCOO^-$	(Schutte et al. 1999)	
1457	ν(CH)	Alkanes	(Colthup 1950), (Fresneau et al. 2017)	
1376	ν(CH)	$HCOO^-$	(Schutte et al. 1999)	
1341	ν(COO^-)	$HCOO^-$	(Schutte et al. 1999)	
1300		?		
1228		?		
1084		Ethylene glycol	(Hudson et al. 2005)	
1050		Ethylene glycol	(Hudson et al. 2005)	
887		Ethylene glycol	(Hudson et al. 2005)	
820		?		
767		$HCOO^-NH4^+$?	(Muñoz Caro & Schutte 2003)	

Note. All species assignments are tentative except the ones in bold.

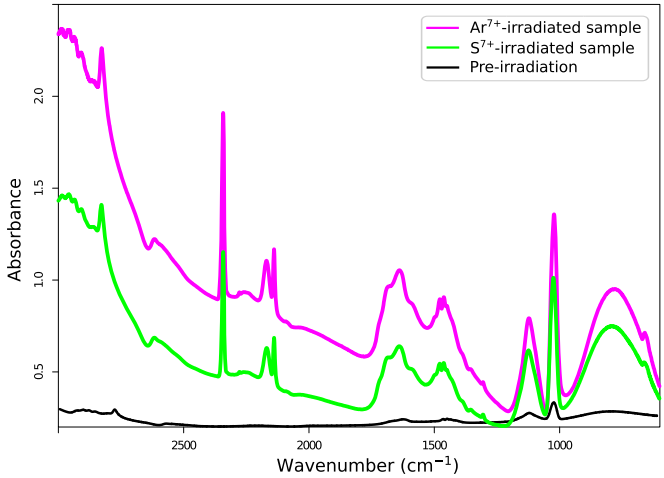

Figure 5. IR spectra of ices (H_2O:CH_3OH:NH_3 ices, 2:1:1), taken at 10 K, one before irradiation (black), one after irradiation by argon (Ar^{7+} ions, magenta), and one after sulfur (S^{7+} ions, green), before warming up. Note that in the pre-irradiation case, only one layer has been deposited, while argon-irradiated and sulfur-irradiated represent 15 and 10 layers, respectively, which explains the difference in absorbance in water, methanol, and ammonia features.

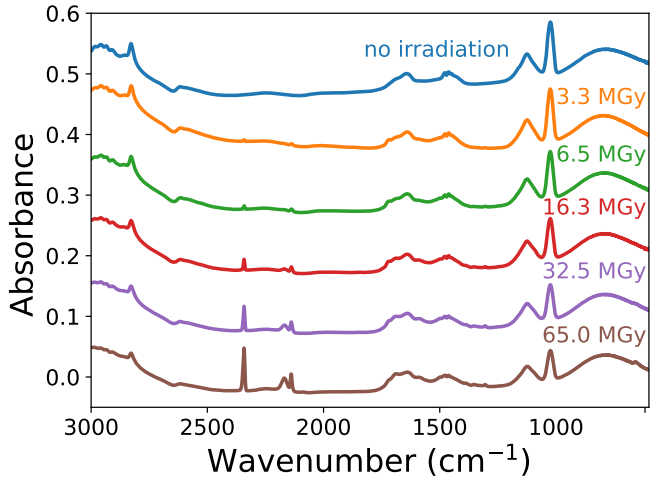

Figure 6. Spectra of the first ice layer at 10 K, irradiated with S^{7+}. From top to bottom: no irradiation, 3.3, 6.5, 16.3, 32.5, and 65.0 MGy. The features of CO_2 at 2340 cm^{-1}, of CO at 2140 cm^{-1}, CH_4 at 1304 cm^{-1}, and OCN^- at 2169 cm^{-1} are evolving with irradiation.

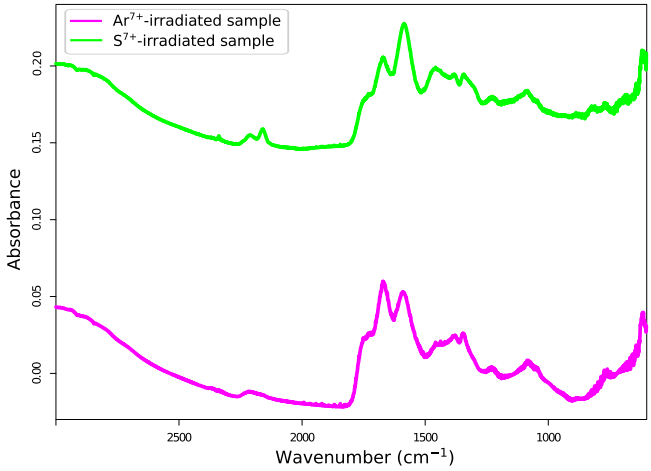

Figure 7. IR spectra of the residue, taken at 300 K, after irradiation by argon (Ar^{7+} ions, magenta) and sulfur (S^{7+} ions, green). The residue resulted from irradiated H_2O:CH_3OH:NH_3 ices (2:1:1).

a trapping of these molecules in the residue. We note that the sulfur-irradiated sample does not appear to display the features of sulfuric acid seen in previous experiments involving sulfur in water ice (Moore et al. 2007; Strazzulla et al. 2007). We attribute this to a much lower sulfur amount present in our experiments (each layer was subjected to a fluence of $\approx 1 \times 10^{14}$ cm^{-2}, to be compared to 3×10^{16} cm^{-2} in the experiments of Strazzulla et al. 2007), along with the presence of NH_3 that makes sulfuric acid features at 1100 cm^{-1} difficult to distinguish. Other possible explanations include the lower temperature of our experiments (although the spectras during heating of the sample, not shown here, do not appear to present sulfuric acid features) or that in the presence of methanol and ammonia sulfur could be mostly incorporated into other products than sulfuric acid.

Appendix B
FT-ICR-MS Data Analysis

Supplementary figures regarding the FT-ICR-MS analysis. In the following, details on data mining of experimental FT-ICR-MS data are given. First, error analysis on formula assignment is reported (Figure 8). Then, distribution of organosulfur (CHNOS) compounds in contrast to CHO and CHNO compounds highlights

Table 3
List of Detected Organosulfur (CHNOS) Molecular Formulas

m/z (exp)	Error (ppm)	Molecular Ion Formula	Intensity/Arbitrary Units	H/C	O/C
147.05974	0.119	C5H12N2OS-	5.05E+06	2.4	0.2
161.00264	−0.016	C4H6N2O3S-	8.10E+06	1.5	0.75
163.0183	−0.077	C4H8N2O3S-	9.97E+06	2	0.75
164.01356	−0.143	C3H7N3O3S-	7.28E+06	2.33	1
166.01796	−0.039	C4H9NO4S-	1.94E+07	2.25	1
172.0186	0.125	C5H7N3O2S-	3.70E+06	1.4	0.4
173.00264	−0.014	C5H6N2O3S-	4.23E+06	1.2	0.6
175.01831	−0.129	C5H8N2O3S-	1.36E+07	1.6	0.6
175.06592	−0.083	C5H12N4OS-	6.07E+06	2.4	0.2
176.99757	−0.099	C4H6N2O4S-	1.27E+07	1.5	1
178.01797	−0.093	C5H9NO4S-	7.47E+06	1.8	0.8
178.0292	−0.076	C4H9N3O3S-	1.37E+07	2.25	0.75
179.01321	−0.042	C4H8N2O4S-	2.31E+07	2	1
180.03361	−0.036	C5H11NO4S-	1.19E+07	2.2	0.8
181.02887	−0.097	C4H10N2O4S-	2.72E+07	2.5	1
188.01354	−0.019	C5H7N3O3S-	1.07E+07	1.4	0.6
189.03394	−0.013	C6H10N2O3S-	1.16E+07	1.67	0.5
189.9928	0.008	C4H5N3O4S-	6.09E+06	1.25	1
190.02921	−0.124	C5H9N3O3S-	1.47E+07	1.8	0.6
191.01322	−0.092	C5H8N2O4S-	3.06E+07	1.6	0.8
192.00848	−0.148	C4H7N3O4S-	1.64E+07	1.75	1
192.03364	−0.19	C6H11NO4S-	7.62E+06	1.83	0.67
192.04484	−0.018	C5H11N3O3S-	1.20E+07	2.2	0.6
193.02887	−0.091	C5H10N2O4S-	3.72E+07	2	0.8
193.0401	−0.075	C4H10N4O3S-	9.04E+06	2.5	0.75
193.06529	−0.272	C6H14N2O3S-	4.64E+06	2.33	0.5
194.01289	−0.111	C5H9NO5S-	1.62E+07	1.8	1
194.02412	−0.095	C4H9N3O4S-	5.39E+07	2.25	1
195.04452	−0.09	C5H12N2O4S-	3.78E+07	2.4	0.8
196.02854	−0.11	C5H11NO5S-	3.29E+07	2.2	1
201.03395	−0.062	C7H10N2O3S-	4.86E+06	1.43	0.43
202.0292	−0.067	C6H9N3O3S-	1.47E+07	1.5	0.5
203.04961	−0.111	C7H12N2O3S-	6.61E+06	1.71	0.43
204.00843	0.105	C5H7N3O4S-	1.67E+07	1.4	0.8
205.02886	−0.037	C6H10N2O4S-	2.34E+07	1.67	0.67
205.04011	−0.119	C5H10N4O3S-	9.80E+06	2	0.6
206.0241	0.007	C5H9N3O4S-	2.96E+07	1.8	0.8
206.06049	−0.017	C6H13N3O3S-	8.91E+06	2.17	0.5
207.01937	−0.094	C4H8N4O4S-	2.44E+07	2	1
207.0445	0.012	C6H12N2O4S-	2.88E+07	2	0.67
207.05574	−0.022	C5H12N4O3S-	1.43E+07	2.4	0.6
208.03976	−0.041	C5H11N3O4S-	4.63E+07	2.2	0.8
209.02378	−0.06	C5H10N2O5S-	5.78E+07	2	1
209.03499	0.05	C4H10N4O4S-	3.81E+07	2.5	1
209.06013	0.108	C6H14N2O4S-	1.80E+07	2.33	0.67
210.00776	0.112	C5H9NO6S-	1.64E+07	1.8	1.2
210.04417	−0.007	C6H13NO5S-	1.79E+07	2.17	0.83
211.03941	0.036	C5H12N2O5S-	3.94E+07	2.4	1
212.02343	0.017	C5H11NO6S-	2.41E+07	2.2	1.2
216.04484	−0.016	C7H11N3O3S-	1.26E+07	1.57	0.43
216.11761	−0.016	C9H19N3OS-	4.44E+06	2.11	0.11
217.00368	0.094	C5H6N4O4S-	4.80E+06	1.2	0.8
217.02889	−0.173	C7H10N2O4S-	9.44E+06	1.43	0.57
217.04011	−0.113	C6H10N4O3S-	9.67E+06	1.67	0.5
218.02409	0.053	C6H9N3O4S-	2.30E+07	1.5	0.67
218.06049	−0.016	C7H13N3O3S-	1.57E+07	1.86	0.43
219.00813	−0.057	C6H8N2O5S-	9.04E+06	1.33	0.83
219.01934	0.048	C5H8N4O4S-	1.42E+07	1.6	0.8
219.04449	0.057	C7H12N2O4S-	1.94E+07	1.71	0.57
219.05572	0.071	C6H12N4O3S-	1.04E+07	2	0.5
220.00337	−0.016	C5H7N3O5S-	1.80E+07	1.4	1
220.02853	−0.052	C7H11NO5S-	7.25E+06	1.57	0.71
220.03975	0.007	C6H11N3O4S-	4.60E+07	1.83	0.67
221.02377	−0.011	C6H10N2O5S-	3.28E+07	1.67	0.83

Table 3
(Continued)

m/z (exp)	Error (ppm)	Molecular Ion Formula	Intensity/Arbitrary Units	H/C	O/C
221.03499	0.048	C5H10N4O4S-	5.46E+07	2	0.8
221.06011	0.192	C7H14N2O4S-	1.78E+07	2	0.57
222.01899	0.119	C5H9N3O5S-	4.42E+07	1.8	1
222.04418	−0.052	C7H13NO5S-	1.10E+07	1.86	0.71
222.05539	0.052	C6H13N3O4S-	4.34E+07	2.17	0.67
223.00299	0.191	C5H8N2O6S-	1.79E+07	1.6	1.2
223.03942	−0.011	C6H12N2O5S-	4.68E+07	2	0.83
223.05063	0.092	C5H12N4O4S-	3.68E+07	2.4	0.8
224.02344	−0.029	C6H11NO6S-	1.44E+07	1.83	1
224.03464	0.118	C5H11N3O5S-	6.53E+07	2.2	1
224.05978	0.172	C7H15NO5S-	1.06E+07	2.14	0.71
225.01865	0.144	C5H10N2O6S-	6.43E+07	2	1.2
225.05505	0.078	C6H14N2O5S-	5.44E+07	2.33	0.83
226.03907	0.06	C6H13NO6S-	2.77E+07	2.17	1
227.03433	0.011	C5H12N2O6S-	1.80E+07	2.4	1.2
228.05475	−0.072	C6H15NO6S-	9.55E+06	2.5	1
229.04007	0.068	C7H10N4O3S-	9.27E+06	1.43	0.43
230.02405	0.224	C7H9N3O4S-	1.00E+07	1.29	0.57
230.06052	−0.146	C8H13N3O3S-	1.03E+07	1.63	0.38
231.01933	0.089	C6H8N4O4S-	1.11E+07	1.33	0.67
231.03058	0.015	C5H8N6O3S-	2.75E+07	1.6	0.6
231.04448	0.097	C8H12N2O4S-	7.78E+06	1.5	0.5
231.05569	0.197	C7H12N4O3S-	1.60E+07	1.71	0.43
232.03974	0.05	C7H11N3O4S-	3.33E+07	1.57	0.57
233.02376	0.032	C7H10N2O5S-	1.59E+07	1.43	0.71
233.03498	0.088	C6H10N4O4S-	2.44E+07	1.67	0.67
233.06016	−0.032	C8H14N2O4S-	1.42E+07	1.75	0.5
233.07136	0.109	C7H14N4O3S-	1.19E+07	2	0.43
234.01899	0.113	C6H9N3O5S-	3.38E+07	1.5	0.83
234.03026	−0.045	C5H9N5O4S-	8.38E+06	1.8	0.8
234.05539	0.049	C7H13N3O4S-	5.57E+07	1.86	0.57
235.00307	−0.16	C6H8N2O6S-	7.38E+06	1.33	1
235.01425	0.066	C5H8N4O5S-	1.46E+07	1.6	1
235.03941	0.032	C7H12N2O5S-	3.82E+07	1.71	0.71
235.05064	0.045	C6H12N4O4S-	7.32E+07	2	0.67
235.07582	−0.074	C8H16N2O4S-	8.59E+06	2	0.5
235.087	0.151	C7H16N4O3S-	4.47E+06	2.29	0.43
235.99828	0.006	C5H7N3O6S-	7.28E+06	1.4	1.2
236.02347	−0.155	C7H11NO6S-	7.20E+06	1.57	0.86
236.03466	0.028	C6H11N3O5S-	8.58E+07	1.83	0.83
236.04588	0.083	C5H11N5O4S-	2.02E+07	2.2	0.8
236.07106	−0.036	C7H15N3O4S-	3.54E+07	2.14	0.57
237.01868	0.011	C6H10N2O6S-	3.75E+07	1.67	1
237.02988	0.15	C5H10N4O5S-	7.56E+07	2	1
237.05504	0.116	C7H14N2O5S-	5.48E+07	2	0.71
237.06629	0.044	C6H14N4O4S-	6.48E+07	2.33	0.67
238.01389	0.174	C5H9N3O6S-	3.65E+07	1.8	1.2
238.03904	0.183	C7H13NO6S-	1.27E+07	1.86	0.86
238.0503	0.069	C6H13N3O5S-	9.16E+07	2.17	0.83
239.03432	0.052	C6H12N2O6S-	7.70E+07	2	1
239.04555	0.065	C5H12N4O5S-	4.86E+07	2.4	1
239.07071	0.031	C7H16N2O5S-	5.86E+07	2.29	0.71
240.01836	−0.048	C6H11NO7S-	1.70E+07	1.83	1.17
240.02956	0.09	C5H11N3O6S-	3.77E+07	2.2	1.2
240.04489	−0.223	C9H11N3O3S-	5.39E+06	1.22	0.33
240.0547	0.14	C7H15NO6S-	1.42E+07	2.14	0.86
240.06597	−0.015	C6H15N3O5S-	2.76E+07	2.5	0.83
241.02234	−0.056	C8H10N4OS2-	4.76E+06	1.25	0.13
241.04008	0.023	C8H10N4O3S-	6.84E+06	1.25	0.38
241.04995	0.135	C6H14N2O6S-	2.96E+07	2.33	1
242.03399	0.035	C6H13NO7S-	1.03E+07	2.17	1.17
242.06045	0.151	C9H13N3O3S-	5.57E+06	1.44	0.33
243.05571	0.105	C8H12N4O3S-	1.13E+07	1.5	0.38
244.03974	0.047	C8H11N3O4S-	1.48E+07	1.38	0.5

Table 3
(Continued)

m/z (exp)	Error (ppm)	Molecular Ion Formula	Intensity/Arbitrary Units	H/C	O/C
245.02379	−0.092	C8H10N2O5S-	6.39E+06	1.25	0.63
245.03498	0.084	C7H10N4O4S-	2.14E+07	1.43	0.57
245.07132	0.267	C8H14N4O3S-	1.18E+07	1.75	0.38
246.01901	0.026	C7H9N3O5S-	1.02E+07	1.29	0.71
246.05538	0.087	C8H13N3O4S-	3.46E+07	1.63	0.5
247.01423	0.144	C6H8N4O5S-	8.15E+06	1.33	0.83
247.03941	0.03	C8H12N2O5S-	1.65E+07	1.5	0.63
247.05067	−0.079	C7H12N4O4S-	3.83E+07	1.71	0.57
247.08698	0.225	C8H16N4O3S-	9.11E+06	2	0.38
248.03465	0.067	C7H11N3O5S-	4.23E+07	1.57	0.71
248.04587	0.119	C6H11N5O4S-	2.65E+07	1.83	0.67
248.07102	0.127	C8H15N3O4S-	4.65E+07	1.88	0.5
248.08227	0.058	C7H15N5O3S-	2.60E+07	2.14	0.43
249.01869	−0.03	C7H10N2O6S-	1.19E+07	1.43	0.86
249.02989	0.102	C6H10N4O5S-	3.71E+07	1.67	0.83
249.05506	0.03	C8H14N2O5S-	2.88E+07	1.75	0.63
249.06627	0.122	C7H14N4O4S-	7.23E+07	2	0.57
250.01393	0.006	C6H9N3O6S-	2.58E+07	1.5	1
250.02516	0.018	C5H9N5O5S-	1.22E+07	1.8	1
250.05032	−0.014	C7H13N3O5S-	1.06E+08	1.86	0.71
250.06153	0.078	C6H13N5O4S-	3.95E+07	2.17	0.67
250.99791	0.149	C6H8N2O7S-	6.73E+06	1.33	1.17
251.00918	0.002	C5H8N4O6S-	9.77E+06	1.6	1.2
251.01655	0.094	C7H12N2O4S2-	6.54E+06	1.71	0.57
251.03433	0.01	C7H12N2O6S-	4.57E+07	1.71	0.86
251.04555	0.062	C6H12N4O5S-	1.12E+08	2	0.83
251.0707	0.07	C8H16N2O5S-	3.09E+07	2	0.63
251.08195	0.002	C7H16N4O4S-	5.37E+07	2.29	0.57
252.0184	−0.204	C7H11NO7S-	8.13E+06	1.57	1
252.02958	0.006	C6H11N3O6S-	6.87E+07	1.83	1
252.04078	0.137	C5H11N5O5S-	3.73E+07	2.2	1
252.05479	−0.224	C8H15NO6S-	8.80E+06	1.88	0.75
252.06595	0.065	C7H15N3O5S-	8.64E+07	2.14	0.71
253.0136	−0.01	C6H10N2O7S-	3.40E+07	1.67	1.17
253.02479	0.16	C5H10N4O6S-	4.40E+07	2	1.2
253.04997	0.049	C7H14N2O6S-	5.25E+07	2	0.86
253.06121	0.022	C6H14N4O5S-	8.22E+07	2.33	0.83
253.08636	0.03	C8H18N2O5S-	1.43E+07	2.25	0.63
254.03396	0.152	C7H13NO7S-	1.26E+07	1.86	1
254.04523	0.006	C6H13N3O6S-	5.19E+07	2.17	1
255.02925	−0.01	C6H12N2O7S-	3.03E+07	2	1.17
255.04046	0.08	C5H12N4O6S-	2.33E+07	2.4	1.2
255.05579	−0.214	C9H12N4O3S-	8.57E+06	1.33	0.33
256.03976	−0.033	C9H11N3O4S-	6.68E+06	1.22	0.44
256.04966	−0.045	C7H15NO7S-	1.71E+07	2.14	1
256.06087	0.045	C6H15N3O6S-	1.39E+07	2.5	1
257.03503	−0.115	C8H10N4O4S-	8.53E+06	1.25	0.5
257.04494	−0.165	C6H14N2O7S-	1.06E+07	2.33	1.17
258.05538	0.083	C9H13N3O4S-	1.65E+07	1.44	0.44
258.06665	−0.06	C8H13N5O3S-	1.41E+07	1.63	0.38
259.05066	−0.037	C8H12N4O4S-	3.38E+07	1.5	0.5
260.03465	0.063	C8H11N3O5S-	2.06E+07	1.38	0.63
260.04588	0.075	C7H11N5O4S-	2.14E+07	1.57	0.57
260.07107	−0.071	C9H15N3O4S-	2.71E+07	1.67	0.44
260.08229	−0.021	C8H15N5O3S-	1.53E+07	1.88	0.38
261.02994	−0.094	C7H10N4O5S-	2.29E+07	1.43	0.71
261.04117	−0.082	C6H10N6O4S-	5.57E+06	1.67	0.67
261.05505	0.067	C9H14N2O5S-	1.45E+07	1.56	0.56
261.06632	−0.075	C8H14N4O4S-	4.95E+07	1.75	0.5
262.01391	0.082	C7H9N3O6S-	1.12E+07	1.29	0.86
262.05034	−0.09	C8H13N3O5S-	5.19E+07	1.63	0.63
262.06155	−0.002	C7H13N5O4S-	4.75E+07	1.86	0.57
262.08675	−0.185	C9H17N3O4S-	2.69E+07	1.89	0.44
263.04555	0.059	C7H12N4O5S-	7.66E+07	1.71	0.71

Table 3
(Continued)

m/z (exp)	Error (ppm)	Molecular Ion Formula	Intensity/Arbitrary Units	H/C	O/C
263.07069	0.105	C9H16N2O5S-	1.92E+07	1.78	0.56
263.08197	−0.074	C8H16N4O4S-	4.88E+07	2	0.5
264.0296	−0.07	C7H11N3O6S-	4.80E+07	1.57	0.86
264.04081	0.017	C6H11N5O5S-	3.89E+07	1.83	0.83
264.06599	−0.089	C8H15N3O5S-	9.44E+07	1.88	0.63
264.07717	0.112	C7H15N5O4S-	3.95E+07	2.14	0.57
265.02484	−0.036	C6H10N4O6S-	3.96E+07	1.67	1
265.05	−0.066	C8H14N2O6S-	4.66E+07	1.75	0.75
265.06122	−0.017	C7H14N4O5S-	1.29E+08	2	0.71
265.08641	−0.16	C9H18N2O5S-	1.68E+07	2	0.56
265.09761	−0.036	C8H18N4O4S-	1.35E+07	2.25	0.5
266.00884	0.024	C6H9N3O7S-	1.83E+07	1.5	1.17
266.02012	−0.152	C5H9N5O6S-	8.59E+06	1.8	1.2
266.03398	0.07	C8H13NO7S-	1.00E+07	1.63	0.88
266.04522	0.043	C7H13N3O6S-	1.22E+08	1.86	0.86
266.05648	−0.058	C6H13N5O5S-	7.34E+07	2.17	0.83
266.08162	−0.013	C8H17N3O5S-	5.40E+07	2.13	0.63
267.02927	−0.084	C7H12N2O7S-	4.16E+07	1.71	1
267.04049	−0.036	C6H12N4O6S-	9.23E+07	2	1
267.05171	0.013	C5H12N6O5S-	1.23E+07	2.4	1
267.06564	−0.028	C8H16N2O6S-	4.85E+07	2	0.75
267.07686	0.021	C7H16N4O5S-	1.00E+08	2.29	0.71
268.0245	−0.013	C6H11N3O7S-	4.58E+07	1.83	1.17
268.03573	−0.002	C5H11N5O6S-	2.24E+07	2.2	1.2
268.04385	−0.285	C15H11NO2S-	7.57E+06	0.73	0.13
268.04974	−0.341	C8H15NO7S-	1.24E+07	1.88	0.88
268.06088	0.006	C7H15N3O6S-	7.93E+07	2.14	0.86
268.07208	0.129	C6H15N5O5S-	1.87E+07	2.5	0.83
269.04493	−0.121	C7H14N2O7S-	3.69E+07	2	1
269.05613	0.002	C6H14N4O6S-	4.46E+07	2.33	1
269.08132	−0.139	C8H18N2O6S-	3.03E+07	2.25	0.75
270.01906	−0.161	C9H9N3O5S-	5.82E+06	1	0.56
270.02891	0.013	C7H13NO8S-	1.10E+07	1.86	1.14
270.03024	0.035	C8H9N5O4S-	5.93E+06	1.13	0.5
270.04015	−0.013	C6H13N3O7S-	2.59E+07	2.17	1.17
270.06662	0.054	C9H13N5O3S-	7.01E+06	1.44	0.33
270.07653	0.006	C7H17N3O6S-	1.76E+07	2.43	0.86
271.05068	−0.109	C9H12N4O4S-	1.57E+07	1.33	0.44
271.06058	−0.12	C7H16N2O7S-	1.31E+07	2.29	1
272.03472	−0.197	C9H11N3O5S-	7.77E+06	1.22	0.56
272.04589	0.035	C8H11N5O4S-	1.33E+07	1.38	0.5
272.05584	−0.16	C6H15N3O7S-	8.60E+06	2.5	1.17
272.08233	−0.167	C9H15N5O3S-	1.48E+07	1.67	0.33
273.0663	0.002	C9H14N4O4S-	3.59E+07	1.56	0.44
274.05033	−0.049	C9H13N3O5S-	2.47E+07	1.44	0.56
274.06157	−0.075	C8H13N5O4S-	3.09E+07	1.63	0.5
275.03433	0.009	C9H12N2O6S-	9.40E+06	1.33	0.67
275.04561	−0.162	C8H12N4O5S-	4.04E+07	1.5	0.63
275.08197	−0.071	C9H16N4O4S-	4.35E+07	1.78	0.44
276.0296	−0.067	C8H11N3O6S-	1.83E+07	1.38	0.75
276.04083	−0.056	C7H11N5O5S-	2.41E+07	1.57	0.71
276.06596	0.024	C9H15N3O5S-	4.87E+07	1.67	0.56
276.07723	−0.11	C8H15N5O4S-	5.54E+07	1.88	0.5
277.02486	−0.106	C7H10N4O6S-	1.66E+07	1.43	0.86
277.05	−0.063	C9H14N2O6S-	1.79E+07	1.56	0.67
277.06125	−0.125	C8H14N4O5S-	9.00E+07	1.75	0.63
277.09767	−0.251	C9H18N4O4S-	2.75E+07	2	0.44
278.00881	0.131	C7H9N3O7S-	7.55E+06	1.29	1
278.04525	−0.067	C8H13N3O6S-	6.21E+07	1.63	0.75
278.05648	−0.056	C7H13N5O5S-	7.89E+07	1.86	0.71
278.08164	−0.085	C9H17N3O5S-	6.45E+07	1.89	0.56
278.09289	−0.146	C8H17N5O4S-	4.21E+07	2.13	0.5
279.02925	−0.009	C8H12N2O7S-	1.32E+07	1.5	0.88
279.0405	−0.07	C7H12N4O6S-	8.68E+07	1.71	0.86

Table 3
(Continued)

m/z (exp)	Error (ppm)	Molecular Ion Formula	Intensity/Arbitrary Units	H/C	O/C
279.05172	−0.023	C6H12N6O5S-	1.48E+07	2	0.83
279.06565	−0.063	C9H16N2O6S-	3.49E+07	1.78	0.67
279.0769	−0.124	C8H16N4O5S-	1.04E+08	2	0.63
280.02449	0.023	C7H11N3O7S-	3.98E+07	1.57	1
280.03577	−0.145	C6H11N5O6S-	3.09E+07	1.83	1
280.06087	0.041	C8H15N3O6S-	1.27E+08	1.88	0.75
280.07211	0.016	C7H15N5O5S-	8.59E+07	2.14	0.71
280.0973	−0.12	C9H19N3O5S-	3.21E+07	2.11	0.56
281.01977	−0.087	C6H10N4O7S-	1.99E+07	1.67	1.17
281.04486	0.133	C8H14N2O7S-	4.11E+07	1.75	0.88
281.05616	−0.105	C7H14N4O6S-	1.20E+08	2	0.86
281.06739	−0.094	C6H14N6O5S-	3.28E+07	2.33	0.83
281.08126	0.08	C9H18N2O6S-	3.23E+07	2	0.67
281.09252	−0.016	C8H18N4O5S-	6.69E+07	2.25	0.63
282.04016	−0.048	C7H13N3O7S-	6.44E+07	1.86	1
282.05141	−0.108	C6H13N5O6S-	4.88E+07	2.17	1
282.07652	0.041	C8H17N3O6S-	7.61E+07	2.13	0.75
283.02412	0.15	C7H12N2O8S-	2.22E+07	1.71	1.14
283.0354	−0.016	C6H12N4O7S-	4.95E+07	2	1.17
283.06055	−0.009	C8H16N2O7S-	3.41E+07	2	0.88
283.07176	0.072	C7H16N4O6S-	5.92E+07	2.29	0.86
283.09694	−0.026	C9H20N2O6S-	9.89E+06	2.22	0.67
284.03462	0.164	C10H11N3O5S-	5.53E+06	1.1	0.5
284.04458	−0.058	C8H15NO8S-	8.69E+06	1.88	1
284.05583	−0.118	C7H15N3O7S-	3.61E+07	2.14	1
284.06702	0.033	C6H15N5O6S-	1.90E+07	2.5	1
284.09215	0.111	C8H19N3O6S-	1.23E+07	2.38	0.75
285.0398	0.044	C7H14N2O8S-	1.52E+07	2	1.14
285.05105	−0.016	C6H14N4O7S-	2.52E+07	2.33	1.17
285.06635	−0.174	C10H14N4O4S-	1.63E+07	1.4	0.4
285.07625	−0.184	C8H18N2O7S-	1.27E+07	2.25	0.88
286.05036	−0.152	C10H13N3O5S-	9.31E+06	1.3	0.5
287.04562	−0.19	C9H12N4O5S-	1.91E+07	1.33	0.56
287.09314	0.152	C9H16N6O3S-	1.50E+07	1.78	0.33
288.02963	−0.168	C9H11N3O6S-	9.35E+06	1.22	0.67
288.04083	−0.054	C8H11N5O5S-	1.54E+07	1.38	0.63
288.06594	0.092	C10H15N3O5S-	2.24E+07	1.5	0.5
288.07722	−0.071	C9H15N5O4S-	4.31E+07	1.67	0.44
289.0612	0.054	C9H14N4O5S-	5.63E+07	1.56	0.56
289.07249	−0.144	C8H14N6O4S-	3.09E+07	1.75	0.5
290.04524	−0.029	C9H13N3O6S-	3.13E+07	1.44	0.67
290.05648	−0.053	C8H13N5O5S-	5.23E+07	1.63	0.63
290.08161	0.022	C10H17N3O5S-	3.86E+07	1.7	0.5
290.09287	−0.071	C9H17N5O4S-	5.15E+07	1.89	0.44
291.04049	−0.033	C8H12N4O6S-	4.39E+07	1.5	0.75
291.05176	−0.16	C7H12N6O5S-	1.91E+07	1.71	0.71
291.07685	0.053	C9H16N4O5S-	9.15E+07	1.78	0.56
291.08808	0.064	C8H16N6O4S-	3.79E+07	2	0.5
292.02451	−0.046	C8H11N3O7S-	1.60E+07	1.38	0.88
292.03573	−0.002	C7H11N5O6S-	2.71E+07	1.57	0.86
292.0609	−0.063	C9H15N3O6S-	6.86E+07	1.67	0.67
292.0721	0.05	C8H15N5O5S-	1.06E+08	1.88	0.63
292.09728	−0.046	C10H19N3O5S-	3.48E+07	1.9	0.5
292.10848	0.067	C9H19N5O4S-	2.78E+07	2.11	0.44
293.04488	0.06	C9H14N2O7S-	1.75E+07	1.56	0.78
293.05614	−0.032	C8H14N4O6S-	1.13E+08	1.75	0.75
293.06741	−0.159	C7H14N6O5S-	4.95E+07	2	0.71
293.08128	0.009	C10H18N2O6S-	1.88E+07	1.8	0.6
293.0925	0.053	C9H18N4O5S-	7.88E+07	2	0.56
294.04017	−0.08	C8H13N3O7S-	5.26E+07	1.63	0.88
294.05141	−0.104	C7H13N5O6S-	9.19E+07	1.86	0.86
294.07654	−0.029	C9H17N3O6S-	9.49E+07	1.89	0.67
294.0878	−0.121	C8H17N5O5S-	8.88E+07	2.13	0.63
295.03541	−0.049	C7H12N4O7S-	5.34E+07	1.71	1

Table 3
(Continued)

m/z (exp)	Error (ppm)	Molecular Ion Formula	Intensity/Arbitrary Units	H/C	O/C
295.0466	0.097	C6H12N6O6S-	1.65E+07	2	1
295.06057	−0.076	C9H16N2O7S-	3.25E+07	1.78	0.78
295.07182	−0.134	C8H16N4O6S-	1.27E+08	2	0.75
295.08304	−0.09	C7H16N6O5S-	2.89E+07	2.29	0.71
296.01947	−0.198	C7H11N3O8S-	2.22E+07	1.57	1.14
296.03069	−0.154	C6H11N5O7S-	1.65E+07	1.83	1.17
296.05578	0.056	C8H15N3O7S-	8.21E+07	1.88	0.88
296.06705	−0.069	C7H15N5O6S-	8.25E+07	2.14	0.86
296.09221	−0.096	C9H19N3O6S-	4.99E+07	2.11	0.67
297.03985	−0.126	C8H14N2O8S-	2.70E+07	1.75	1
297.05108	−0.116	C7H14N4O7S-	7.23E+07	2	1
297.06228	−0.005	C6H14N6O6S-	2.99E+07	2.33	1
297.06637	−0.234	C11H14N4O4S-	7.63E+06	1.27	0.36
297.0762	−0.008	C9H18N2O7S-	3.31E+07	2	0.78
297.08746	−0.099	C8H18N4O6S-	6.92E+07	2.25	0.75
298.03506	0.005	C7H13N3O8S-	3.55E+07	1.86	1.14
298.0463	−0.018	C6H13N5O7S-	2.85E+07	2.17	1.17
298.06158	−0.102	C10H13N5O4S-	1.15E+07	1.3	0.4
298.07148	−0.112	C8H17N3O7S-	4.39E+07	2.13	0.88
298.08267	0.032	C7H17N5O6S-	2.30E+07	2.43	0.86
299.04556	0.018	C10H12N4O5S-	1.02E+07	1.2	0.5
299.05546	0.008	C8H16N2O8S-	1.90E+07	2	1
299.06672	−0.082	C7H16N4O7S-	2.95E+07	2.29	1
300.05075	−0.128	C7H15N3O8S-	1.86E+07	2.14	1.14
300.06196	−0.052	C6H15N5O7S-	1.90E+07	2.5	1.17
300.07724	−0.135	C10H15N5O4S-	2.35E+07	1.5	0.4
301.06123	−0.048	C10H14N4O5S-	2.60E+07	1.4	0.5
301.99439	0.227	C6H13N3O5S3-	6.19E+06	2.17	0.83
302.05649	−0.084	C9H13N5O5S-	2.90E+07	1.44	0.56
303.04049	−0.031	C9H12N4O6S-	1.75E+07	1.33	0.67
303.07689	−0.081	C10H16N4O5S-	5.15E+07	1.6	0.5
303.08813	−0.104	C9H16N6O4S-	3.71E+07	1.78	0.44
304.06087	0.038	C10H15N3O6S-	2.81E+07	1.5	0.6
304.07212	−0.018	C9H15N5O5S-	6.70E+07	1.67	0.56
305.05615	−0.064	C9H14N4O6S-	6.05E+07	1.56	0.67
305.06743	−0.218	C8H14N6O5S-	3.99E+07	1.75	0.63
306.04014	0.021	C9H13N3O7S-	2.40E+07	1.44	0.78
306.05141	−0.1	C8H13N5O6S-	5.35E+07	1.63	0.75
306.07656	−0.093	C10H17N3O6S-	5.61E+07	1.7	0.6
306.08776	0.015	C9H17N5O5S-	1.04E+08	1.89	0.56
307.03543	−0.112	C8H12N4O7S-	3.51E+07	1.5	0.88
307.07183	−0.161	C9H16N4O6S-	1.23E+08	1.78	0.67
307.08306	−0.151	C8H16N6O5S-	7.49E+07	2	0.63
308.03065	−0.018	C7H11N5O7S-	1.40E+07	1.57	1
308.05584	−0.141	C9H15N3O7S-	6.47E+07	1.67	0.78
308.06703	−0.002	C8H15N5O6S-	1.18E+08	1.88	0.75
308.07826	0.008	C7H15N7O5S-	1.83E+07	2.14	0.71
308.0922	−0.06	C10H19N3O6S-	6.57E+07	1.9	0.6
308.10345	−0.115	C9H19N5O5S-	7.63E+07	2.11	0.56
308.11735	−0.054	C12H23NO6S-	3.28E+07	1.92	0.5
309.05109	−0.144	C8H14N4O7S-	9.45E+07	1.75	0.88
309.06234	−0.199	C7H14N6O6S-	5.53E+07	2	0.86
309.07621	−0.04	C10H18N2O7S-	2.34E+07	1.8	0.7
309.08743	0.002	C9H18N4O6S-	1.10E+08	2	0.67
310.03507	−0.027	C8H13N3O8S-	3.35E+07	1.63	1
310.04634	−0.147	C7H13N5O7S-	6.10E+07	1.86	1
310.07147	−0.076	C9H17N3O7S-	9.80E+07	1.89	0.78
310.08271	−0.098	C8H17N5O6S-	1.01E+08	2.13	0.75
311.03038	−0.223	C7H12N4O8S-	3.37E+07	1.71	1.14
311.05549	−0.088	C9H16N2O8S-	2.32E+07	1.78	0.89
311.06667	0.082	C8H16N4O7S-	1.02E+08	2	0.88
311.07791	0.059	C7H16N6O6S-	4.21E+07	2.29	0.86
312.05076	−0.155	C8H15N3O8S-	5.75E+07	1.88	1
312.06197	−0.082	C7H15N5O7S-	6.13E+07	2.14	1

Table 3
(Continued)

m/z (exp)	Error (ppm)	Molecular Ion Formula	Intensity/Arbitrary Units	H/C	O/C
312.08712	−0.075	C9H19N3O7S-	4.34E+07	2.11	0.78
313.04602	−0.19	C7H14N4O8S-	6.14E+07	2	1.14
313.05728	−0.276	C6H14N6O7S-	2.34E+07	2.33	1.17
313.08232	0.081	C8H18N4O7S-	3.38E+07	2.25	0.88
313.11877	−0.126	C9H22N4O6S-	1.89E+07	2.44	0.67
314.06638	−0.059	C8H17N3O8S-	2.46E+07	2.13	1
314.07763	−0.113	C7H17N5O7S-	2.71E+07	2.43	1
315.07684	0.081	C11H16N4O5S-	3.39E+07	1.45	0.45
315.08816	−0.195	C10H16N6O4S-	3.48E+07	1.6	0.4
316.01005	0.185	C7H15N3O5S3-	1.15E+07	2.14	0.71
316.07213	−0.049	C10H15N5O5S-	4.92E+07	1.5	0.5
317.05612	0.033	C10H14N4O6S-	3.38E+07	1.4	0.6
317.09252	−0.014	C11H18N4O5S-	5.29E+07	1.64	0.45
317.10377	−0.068	C10H18N6O4S-	4.13E+07	1.8	0.4
318.05139	−0.033	C9H13N5O6S-	3.21E+07	1.44	0.67
318.07657	−0.121	C11H17N3O6S-	3.14E+07	1.55	0.55
319.03543	−0.108	C9H12N4O7S-	1.65E+07	1.33	0.78
319.04666	−0.099	C8H12N6O6S-	1.68E+07	1.5	0.75
319.0718	−0.061	C10H16N4O6S-	8.22E+07	1.6	0.6
319.08307	−0.177	C9H16N6O5S-	7.62E+07	1.78	0.56
319.10815	0.049	C11H20N4O5S-	5.19E+07	1.82	0.45
320.05589	−0.292	C10H15N3O7S-	3.72E+07	1.5	0.7
320.06708	−0.158	C9H15N5O6S-	9.79E+07	1.67	0.67
320.10343	−0.048	C10H19N5O5S-	9.50E+07	1.9	0.5
321.05102	0.079	C9H14N4O7S-	6.06E+07	1.56	0.78
321.06225	0.089	C8H14N6O6S-	5.50E+07	1.75	0.75
321.0875	−0.216	C10H18N4O6S-	1.27E+08	1.8	0.6
321.09873	−0.207	C9H18N6O5S-	8.74E+07	2	0.56
322.03502	0.129	C9H13N3O8S-	1.81E+07	1.44	0.89
322.04628	0.045	C8H13N5O7S-	4.81E+07	1.63	0.88
322.07153	−0.259	C10H17N3O7S-	7.34E+07	1.7	0.7
322.08274	−0.188	C9H17N5O6S-	1.57E+08	1.89	0.67
322.11903	0.107	C10H21N5O5S-	4.61E+07	2.1	0.5
323.06677	−0.231	C9H16N4O7S-	1.31E+08	1.78	0.78
323.07797	−0.128	C8H16N6O6S-	1.03E+08	2	0.75
323.10307	0.032	C10H20N4O6S-	9.03E+07	2	0.6
324.05078	−0.211	C9H15N3O8S-	5.12E+07	1.67	0.89
324.06202	−0.233	C8H15N5O7S-	1.19E+08	1.88	0.88
324.07322	−0.131	C7H15N7O6S-	2.50E+07	2.14	0.86
324.08708	0.051	C10H19N3O7S-	7.70E+07	1.9	0.7
324.09833	−0.002	C9H19N5O6S-	1.10E+08	2.11	0.67
325.046	−0.122	C8H14N4O8S-	6.26E+07	1.75	1
325.05727	−0.235	C7H14N6O7S-	4.39E+07	2	1
325.07117	−0.177	C10H18N2O8S-	2.38E+07	1.8	0.8
325.08239	−0.137	C9H18N4O7S-	1.15E+08	2	0.78
325.09358	−0.005	C8H18N6O6S-	5.14E+07	2.25	0.75
326.02996	0.051	C8H13N3O9S-	2.19E+07	1.63	1.13
326.0412	0.029	C7H13N5O8S-	3.18E+07	1.86	1.14
326.0664	−0.118	C9H17N3O8S-	6.34E+07	1.89	0.89
326.07768	−0.262	C8H17N5O7S-	9.97E+07	2.13	0.88
326.10276	−0.041	C10H21N3O7S-	3.75E+07	2.1	0.7
327.05038	−0.008	C9H16N2O9S-	1.57E+07	1.78	1
327.06159	0.063	C8H16N4O8S-	6.52E+07	2	1
327.07279	0.164	C7H16N6O7S-	4.94E+07	2.29	1
328.04562	0.02	C8H15N3O9S-	3.13E+07	1.88	1.13
328.0569	−0.123	C7H15N5O8S-	5.14E+07	2.14	1.14
328.0722	−0.261	C11H15N5O5S-	2.85E+07	1.36	0.45
329.0562	−0.211	C11H14N4O6S-	1.71E+07	1.27	0.55
329.06741	−0.141	C10H14N6O5S-	2.23E+07	1.4	0.5
329.07723	0.093	C8H18N4O8S-	2.85E+07	2.25	1
331.02098	0.083	C7H16N4O5S3-	8.73E+06	2.29	0.71
331.07176	0.062	C11H16N4O6S-	4.11E+07	1.45	0.55
331.08301	0.011	C10H16N6O5S-	5.63E+07	1.6	0.5
332.06702	0.029	C10H15N5O6S-	5.01E+07	1.5	0.6

Table 3
(Continued)

m/z (exp)	Error (ppm)	Molecular Ion Formula	Intensity/Arbitrary Units	H/C	O/C
332.07822	0.128	C9H15N7O5S-	2.60E+07	1.67	0.56
332.10344	−0.077	C11H19N5O5S-	8.17E+07	1.73	0.45
333.05107	−0.074	C10H14N4O7S-	2.69E+07	1.4	0.7
333.06231	−0.095	C9H14N6O6S-	3.87E+07	1.56	0.67
333.0874	0.092	C11H18N4O6S-	7.46E+07	1.64	0.55
334.04628	0.043	C9H13N5O7S-	2.74E+07	1.44	0.78
334.0827	−0.061	C10H17N5O6S-	1.21E+08	1.7	0.6
335.06671	−0.043	C10H16N4O7S-	8.51E+07	1.6	0.7
335.07791	0.055	C9H16N6O6S-	9.80E+07	1.78	0.67
335.10307	0.031	C11H20N4O6S-	9.44E+07	1.82	0.55
335.11437	−0.169	C10H20N6O5S-	7.49E+07	2	0.5
336.05074	−0.085	C10H15N3O8S-	2.79E+07	1.5	0.8
336.06199	−0.135	C9H15N5O7S-	9.30E+07	1.67	0.78
336.0871	−0.01	C11H19N3O7S-	5.68E+07	1.73	0.64
336.09833	−0.001	C10H19N5O6S-	1.43E+08	1.9	0.6
337.04596	0.001	C9H14N4O8S-	4.21E+07	1.56	0.89
337.05722	−0.079	C8H14N6O7S-	4.47E+07	1.75	0.88
337.08242	−0.221	C10H18N4O7S-	1.29E+08	1.8	0.7
337.09363	−0.153	C9H18N6O6S-	1.27E+08	2	0.67
338.06635	0.034	C10H17N3O8S-	4.99E+07	1.7	0.8
338.07759	0.013	C9H17N5O7S-	1.40E+08	1.89	0.78
338.08884	−0.037	C8H17N7O6S-	5.17E+07	2.13	0.75
338.10275	−0.01	C11H21N3O7S-	4.98E+07	1.91	0.64
338.11402	−0.12	C10H21N5O6S-	8.91E+07	2.1	0.6
339.06166	−0.146	C9H16N4O8S-	8.54E+07	1.78	0.89
339.07291	−0.196	C8H16N6O7S-	9.22E+07	2	0.88
339.098	−0.013	C10H20N4O7S-	8.89E+07	2	0.7
339.10921	0.055	C9H20N6O6S-	5.23E+07	2.22	0.67
340.05689	−0.09	C8H15N5O8S-	7.39E+07	1.88	1
340.06808	0.037	C7H15N7O7S-	2.06E+07	2.14	1
340.08201	0.004	C10H19N3O8S-	5.99E+07	1.9	0.8
340.09325	−0.016	C9H19N5O7S-	9.13E+07	2.11	0.78
341.04084	0.104	C8H14N4O9S-	3.60E+07	1.75	1.13
341.05208	0.084	C7H14N6O8S-	2.18E+07	2	1.14
341.07726	0.001	C9H18N4O8S-	7.30E+07	2	0.89
341.08852	−0.078	C8H18N6O7S-	5.96E+07	2.25	0.88
342.06135	−0.215	C9H17N3O9S-	3.39E+07	1.89	1
342.07257	−0.177	C8H17N5O8S-	6.76E+07	2.13	1
342.08379	−0.139	C7H17N7O7S-	2.90E+07	2.43	1
342.08779	−0.075	C12H17N5O5S-	3.01E+07	1.42	0.42
343.0566	−0.217	C8H16N4O9S-	4.66E+07	2	1.13
343.06784	−0.238	C7H16N6O8S-	3.21E+07	2.29	1.14
344.06711	−0.234	C11H15N5O6S-	3.11E+07	1.36	0.55
344.07698	−0.155	C9H19N3O9S-	2.23E+07	2.11	1
345.08739	0.117	C12H18N4O6S-	3.84E+07	1.5	0.5
345.09865	0.039	C11H18N6O5S-	6.37E+07	1.64	0.45
346.08273	−0.146	C11H17N5O6S-	7.26E+07	1.55	0.55
346.09396	−0.137	C10H17N7O5S-	4.46E+07	1.7	0.5
347.06671	−0.042	C11H16N4O7S-	3.83E+07	1.45	0.64
347.07795	−0.062	C10H16N6O6S-	6.55E+07	1.6	0.6
347.10304	0.117	C12H20N4O6S-	5.80E+07	1.67	0.5
348.06197	−0.073	C10H15N5O7S-	4.58E+07	1.5	0.7
348.09833	−0.001	C11H19N5O6S-	1.11E+08	1.73	0.55
348.10961	−0.136	C10H19N7O5S-	6.18E+07	1.9	0.5
349.08237	−0.07	C11H18N4O7S-	8.40E+07	1.64	0.64
349.0936	−0.062	C10H18N6O6S-	1.22E+08	1.8	0.6
350.0776	−0.016	C10H17N5O7S-	1.13E+08	1.7	0.7
350.08885	−0.064	C9H17N7O6S-	7.01E+07	1.89	0.67
350.11399	−0.03	C11H21N5O6S-	1.07E+08	1.91	0.55
351.06168	−0.198	C10H16N4O8S-	6.32E+07	1.6	0.8
351.0729	−0.161	C9H16N6O7S-	8.97E+07	1.78	0.78
351.09799	0.016	C11H20N4O7S-	1.00E+08	1.82	0.64
351.10921	0.053	C10H20N6O6S-	1.08E+08	2	0.6
352.05686	−0.001	C9H15N5O8S-	5.96E+07	1.67	0.89

Table 3
(Continued)

m/z (exp)	Error (ppm)	Molecular Ion Formula	Intensity/Arbitrary Units	H/C	O/C
352.08197	0.118	C11H19N3O8S-	4.53E+07	1.73	0.73
352.09323	0.041	C10H19N5O7S-	1.43E+08	1.9	0.7
352.10452	−0.121	C9H19N7O6S-	6.70E+07	2.11	0.67
353.04087	0.016	C9H14N4O9S-	2.11E+07	1.56	1
353.05208	0.081	C8H14N6O8S-	2.66E+07	1.75	1
353.07729	−0.084	C10H18N4O8S-	9.30E+07	1.8	0.8
353.08856	−0.188	C9H18N6O7S-	1.24E+08	2	0.78
354.06134	−0.179	C10H17N3O9S-	3.24E+07	1.7	0.9
354.07257	−0.171	C9H17N5O8S-	1.04E+08	1.89	0.89
354.08381	−0.191	C8H17N7O7S-	5.49E+07	2.13	0.88
354.09767	−0.024	C11H21N3O8S-	4.15E+07	1.91	0.73
354.10889	0.013	C10H21N5O7S-	8.20E+07	2.1	0.7
355.05656	−0.097	C9H16N4O9S-	5.41E+07	1.78	1
355.06782	−0.173	C8H16N6O8S-	6.95E+07	2	1
355.08305	−0.103	C12H16N6O5S-	1.73E+07	1.33	0.42
355.09289	0.058	C10H20N4O8S-	6.75E+07	2	0.8
355.10412	0.066	C9H20N6O7S-	6.33E+07	2.22	0.78
356.05183	−0.156	C8H15N5O9S-	3.79E+07	1.88	1.13
356.07696	−0.094	C10H19N3O9S-	3.80E+07	1.9	0.9
356.08818	−0.058	C9H19N5O8S-	7.78E+07	2.11	0.89
356.09938	0.035	C8H19N7O7S-	2.94E+07	2.38	0.88
357.07219	−0.041	C9H18N4O9S-	5.05E+07	2	1
357.08342	−0.032	C8H18N6O8S-	5.23E+07	2.25	1
357.09863	0.094	C12H18N6O5S-	3.54E+07	1.5	0.42
358.05623	−0.108	C9H17N3O10S-	2.03E+07	1.89	1.11
358.06747	−0.127	C8H17N5O9S-	3.91E+07	2.13	1.13
359.07799	−0.171	C11H16N6O6S-	3.93E+07	1.45	0.55
359.08782	0.015	C9H20N4O9S-	2.46E+07	2.22	1
360.06194	0.012	C11H15N5O7S-	2.06E+07	1.36	0.64
360.09833	−0.001	C12H19N5O6S-	6.78E+07	1.58	0.5
360.10961	−0.132	C11H19N7O5S-	5.56E+07	1.73	0.45
361.09355	0.079	C11H18N6O6S-	8.19E+07	1.64	0.55
362.07767	−0.209	C11H17N5O7S-	6.41E+07	1.55	0.64
362.08891	−0.228	C10H17N7O6S-	5.73E+07	1.7	0.6
363.07284	0.01	C10H16N6O7S-	5.50E+07	1.6	0.7
363.09798	0.043	C12H20N4O7S-	6.49E+07	1.67	0.58
363.10926	−0.087	C11H20N6O6S-	1.18E+08	1.82	0.55
364.05692	−0.166	C10H15N5O8S-	3.06E+07	1.5	0.8
364.09326	−0.043	C11H19N5O7S-	1.19E+08	1.73	0.64
364.1045	−0.062	C10H19N7O6S-	8.94E+07	1.9	0.6
365.07723	0.084	C11H18N4O8S-	6.31E+07	1.64	0.73
365.08846	0.092	C10H18N6O7S-	1.21E+08	1.8	0.7
365.11359	0.152	C12H22N4O7S-	7.21E+07	1.83	0.58
365.12488	−0.004	C11H22N6O6S-	8.97E+07	2	0.55
366.07253	−0.056	C10H17N5O8S-	8.86E+07	1.7	0.8
366.08378	−0.102	C9H17N7O7S-	6.65E+07	1.89	0.78
366.09764	0.059	C12H21N3O8S-	3.56E+07	1.75	0.67
366.10893	−0.097	C11H21N5O7S-	1.29E+08	1.91	0.64
366.12015	−0.061	C10H21N7O6S-	6.62E+07	2.1	0.6
367.06781	−0.14	C9H16N6O8S-	6.73E+07	1.78	0.89
367.09291	0.001	C11H20N4O8S-	8.60E+07	1.82	0.73
367.10414	0.01	C10H20N6O7S-	1.19E+08	2	0.7
368.0518	−0.069	C9H15N5O9S-	3.32E+07	1.67	1
368.07691	0.045	C11H19N3O9S-	2.97E+07	1.73	0.82
368.08814	0.053	C10H19N5O8S-	1.13E+08	1.9	0.8
368.09937	0.061	C9H19N7O7S-	7.25E+07	2.11	0.78
369.07215	0.069	C10H18N4O9S-	5.42E+07	1.8	0.9
369.08339	0.05	C9H18N6O8S-	9.72E+07	2	0.89
370.05616	0.085	C10H17N3O10S-	1.33E+07	1.7	1
370.06739	0.093	C9H17N5O9S-	5.89E+07	1.89	1
370.07862	0.101	C8H17N7O8S-	3.75E+07	2.13	1
370.1038	0.026	C10H21N5O8S-	6.47E+07	2.1	0.8
371.05139	0.136	C9H16N4O10S-	2.14E+07	1.78	1.11
371.06264	0.09	C8H16N6O9S-	3.08E+07	2	1.13

Table 3
(Continued)

m/z (exp)	Error (ppm)	Molecular Ion Formula	Intensity/Arbitrary Units	H/C	O/C
371.08776	0.177	C10H20N4O9S-	4.43E+07	2	0.9
371.09901	0.131	C9H20N6O8S-	5.90E+07	2.22	0.89
372.08303	0.12	C9H19N5O9S-	5.16E+07	2.11	1
373.07824	0.224	C8H18N6O9S-	2.05E+07	2.25	1.13
373.09352	0.157	C12H18N6O6S-	4.47E+07	1.5	0.5
375.07291	−0.177	C11H16N6O7S-	2.92E+07	1.45	0.64
375.10924	−0.031	C12H20N6O6S-	8.50E+07	1.67	0.5
376.09322	0.065	C12H19N5O7S-	7.05E+07	1.58	0.58
377.07727	−0.025	C12H18N4O8S-	2.89E+07	1.5	0.67
377.0885	−0.017	C11H18N6O7S-	8.31E+07	1.64	0.64
377.09973	−0.009	C10H18N8O6S-	3.41E+07	1.8	0.6
378.07253	−0.054	C11H17N5O8S-	5.02E+07	1.55	0.73
378.08377	−0.073	C10H17N7O7S-	5.65E+07	1.7	0.7
378.10891	−0.041	C12H21N5O7S-	1.07E+08	1.75	0.58
379.0678	−0.109	C10H16N6O8S-	4.39E+07	1.6	0.8
379.09287	0.107	C12H20N4O8S-	5.68E+07	1.67	0.67
379.1041	0.115	C11H20N6O7S-	1.36E+08	1.82	0.64
380.08821	−0.133	C11H19N5O8S-	1.04E+08	1.73	0.73
380.09947	−0.204	C10H19N7O7S-	1.02E+08	1.9	0.7
380.12453	0.038	C12H23N5O7S-	8.49E+07	1.92	0.58
380.13576	0.046	C11H23N7O6S-	4.73E+07	2.09	0.55
381.07221	−0.091	C11H18N4O9S-	4.35E+07	1.64	0.82
381.08345	−0.109	C10H18N6O8S-	9.82E+07	1.8	0.8
381.09468	−0.101	C9H18N8O7S-	3.67E+07	2	0.78
381.1085	0.159	C12H22N4O8S-	6.36E+07	1.83	0.67
381.11973	0.167	C11H22N6O7S-	1.01E+08	2	0.64
382.0674	0.064	C10H17N5O9S-	5.40E+07	1.7	0.9
382.0786	0.15	C9H17N7O8S-	4.79E+07	1.89	0.89
382.10377	0.103	C11H21N5O8S-	1.03E+08	1.91	0.73
382.11504	0.007	C10H21N7O7S-	8.17E+07	2.1	0.7
383.0627	−0.069	C9H16N6O9S-	3.12E+07	1.78	1
383.08784	−0.038	C11H20N4O9S-	5.78E+07	1.82	0.82
383.09912	−0.161	C10H20N6O8S-	1.11E+08	2	0.8
383.11036	−0.179	C9H20N8O7S-	3.65E+07	2.22	0.78
384.08311	−0.092	C10H19N5O9S-	8.04E+07	1.9	0.9
384.09437	−0.163	C9H19N7O8S-	6.55E+07	2.11	0.89
384.11944	0.051	C11H23N5O8S-	5.11E+07	2.09	0.73
385.06708	0.027	C10H18N4O10S-	2.89E+07	1.8	1
385.07837	−0.121	C9H18N6O9S-	5.77E+07	2	1
386.06229	0.128	C9H17N5O10S-	2.55E+07	1.89	1.11
386.07352	0.136	C8H17N7O9S-	1.73E+07	2.13	1.13
386.09866	0.167	C10H21N5O9S-	5.20E+07	2.1	0.9
386.10992	0.097	C9H21N7O8S-	2.90E+07	2.33	0.89
387.08265	0.234	C10H20N4O10S-	2.69E+07	2	1
387.09391	0.164	C9H20N6O9S-	3.19E+07	2.22	1
388.09316	0.218	C13H19N5O7S-	3.37E+07	1.46	0.54
388.10444	0.097	C12H19N7O6S-	4.68E+07	1.58	0.5
389.08847	0.06	C12H18N6O7S-	4.28E+07	1.5	0.58
389.0997	0.068	C11H18N8O6S-	2.73E+07	1.64	0.55
390.07258	−0.181	C12H17N5O8S-	2.41E+07	1.42	0.67
390.10882	0.191	C13H21N5O7S-	6.00E+07	1.62	0.54
390.12007	0.147	C12H21N7O6S-	7.81E+07	1.75	0.5
391.06788	−0.311	C11H16N6O8S-	2.29E+07	1.45	0.73
391.10416	−0.042	C12H20N6O7S-	9.79E+07	1.67	0.58
392.08821	−0.129	C12H19N5O8S-	6.02E+07	1.58	0.67
392.09946	−0.172	C11H19N7O7S-	8.35E+07	1.73	0.64
392.12447	0.19	C13H23N5O7S-	7.73E+07	1.77	0.54
393.08338	0.073	C11H18N6O8S-	6.67E+07	1.64	0.73
393.09465	−0.022	C10H18N8O7S-	3.47E+07	1.8	0.7
393.10849	0.179	C13H22N4O8S-	4.46E+07	1.69	0.62
393.11982	−0.067	C12H22N6O7S-	1.24E+08	1.83	0.58
393.13109	−0.162	C11H22N8O6S-	5.30E+07	2	0.55
394.06747	−0.115	C11H17N5O9S-	3.05E+07	1.55	0.82
394.0787	−0.108	C10H17N7O8S-	3.52E+07	1.7	0.8

Table 3
(Continued)

m/z (exp)	Error (ppm)	Molecular Ion Formula	Intensity/Arbitrary Units	H/C	O/C
394.10379	0.049	C12H21N5O8S-	8.88E+07	1.75	0.67
394.11504	0.006	C11H21N7O7S-	1.04E+08	1.91	0.64
395.08786	−0.087	C12H20N4O9S-	4.31E+07	1.67	0.75
395.09912	−0.156	C11H20N6O8S-	1.17E+08	1.82	0.73
395.11038	−0.224	C10H20N8O7S-	6.00E+07	2	0.7
395.13542	0.059	C12H24N6O7S-	6.93E+07	2	0.58
396.08303	0.112	C11H19N5O9S-	6.24E+07	1.73	0.82
396.09427	0.095	C10H19N7O8S-	7.74E+07	1.9	0.8
396.11945	0.024	C12H23N5O8S-	7.21E+07	1.92	0.67
396.13069	0.006	C11H23N7O7S-	6.57E+07	2.09	0.64
397.07836	−0.092	C10H18N6O9S-	5.88E+07	1.8	0.9
397.10354	−0.162	C12H22N4O9S-	4.63E+07	1.83	0.75
397.11473	−0.054	C11H22N6O8S-	9.81E+07	2	0.73
398.07353	0.107	C9H17N7O9S-	2.32E+07	1.89	1
398.09868	0.112	C11H21N5O9S-	6.97E+07	1.91	0.82
398.10994	0.044	C10H21N7O8S-	7.77E+07	2.1	0.8
399.0828	−0.149	C11H20N4O10S-	3.00E+07	1.82	0.91
399.09405	−0.192	C10H20N6O9S-	7.53E+07	2	0.9
399.10527	−0.159	C9H20N8O8S-	3.36E+07	2.22	0.89
400.07797	0.049	C10H19N5O10S-	3.65E+07	1.9	1
400.08925	−0.069	C9H19N7O9S-	3.68E+07	2.11	1
400.11436	0.036	C11H23N5O9S-	4.33E+07	2.09	0.82
401.07319	0.121	C9H18N6O10S-	1.86E+07	2	1.11
403.10409	0.133	C13H20N6O7S-	4.42E+07	1.54	0.54
403.11532	0.14	C12H20N8O6S-	3.86E+07	1.67	0.5
404.09935	0.105	C12H19N7O7S-	4.51E+07	1.58	0.58
404.18033	−0.306	C24H27N3OS-	1.15E+08	1.13	0.04
405.11975	0.107	C13H22N6O7S-	8.26E+07	1.69	0.54
406.10382	−0.026	C13H21N5O8S-	5.45E+07	1.62	0.62
406.11511	−0.166	C12H21N7O7S-	9.77E+07	1.75	0.58
407.09912	−0.151	C12H20N6O8S-	7.76E+07	1.67	0.67
407.11038	−0.217	C11H20N8O7S-	6.03E+07	1.82	0.64
408.08306	0.036	C12H19N5O9S-	3.65E+07	1.58	0.75
408.09436	−0.129	C11H19N7O8S-	6.36E+07	1.73	0.73
408.11948	−0.05	C13H23N5O8S-	6.77E+07	1.77	0.62
408.13073	−0.092	C12H23N7O7S-	9.58E+07	1.92	0.58
409.07835	−0.065	C11H18N6O9S-	3.58E+07	1.64	0.82
409.1035	−0.06	C13H22N4O9S-	3.50E+07	1.69	0.69
409.11477	−0.15	C12H22N6O8S-	1.04E+08	1.83	0.67
409.12604	−0.241	C11H22N8O7S-	6.37E+07	2	0.64
410.09875	−0.062	C12H21N5O9S-	6.44E+07	1.75	0.75
410.11002	−0.152	C11H21N7O8S-	9.73E+07	1.91	0.73
411.08268	0.147	C12H20N4O10S-	2.19E+07	1.67	0.83
411.09395	0.057	C11H20N6O9S-	7.16E+07	1.82	0.82
411.10522	−0.033	C10H20N8O8S-	4.81E+07	2	0.8
411.11912	0.013	C13H24N4O9S-	3.00E+07	1.85	0.69
411.1304	−0.101	C12H24N6O8S-	7.32E+07	2	0.67
411.14164	−0.118	C11H24N8O7S-	2.98E+07	2.18	0.64
412.08922	0.006	C10H19N7O9S-	4.68E+07	1.9	0.9
412.11434	0.084	C12H23N5O9S-	5.76E+07	1.92	0.75
412.1256	0.018	C11H23N7O8S-	6.89E+07	2.09	0.73
413.07323	0.021	C10H18N6O10S-	2.15E+07	1.8	1
413.10964	−0.04	C11H22N6O9S-	6.97E+07	2	0.82
414.09368	−0.098	C11H21N5O10S-	3.99E+07	1.91	0.91
414.10497	−0.235	C10H21N7O9S-	5.07E+07	2.1	0.9
414.12011	0.042	C14H21N7O6S-	2.72E+07	1.5	0.43
417.11972	0.176	C14H22N6O7S-	3.93E+07	1.57	0.5
418.11509	−0.114	C13H21N7O7S-	5.50E+07	1.62	0.54
419.11032	−0.068	C12H20N8O7S-	3.46E+07	1.67	0.58
420.09431	−0.006	C12H19N7O8S-	3.40E+07	1.58	0.67
420.13075	−0.137	C13H23N7O7S-	7.58E+07	1.77	0.54
420.17519	−0.163	C24H27N3O2S-	1.45E+08	1.13	0.08
421.07845	−0.3	C12H18N6O9S-	1.88E+07	1.5	0.75
421.08967	−0.27	C11H18N8O8S-	1.66E+07	1.64	0.73

Table 3
(Continued)

m/z (exp)	Error (ppm)	Molecular Ion Formula	Intensity/Arbitrary Units	H/C	O/C
421.11472	−0.027	C13H22N6O8S-	6.60E+07	1.69	0.62
421.12591	0.075	C12H22N8O7S-	6.32E+07	1.83	0.58
422.09871	0.034	C13H21N5O9S-	3.84E+07	1.62	0.69
422.10994	0.041	C12H21N7O8S-	7.54E+07	1.75	0.67
422.14628	0.148	C13H25N7O7S-	6.72E+07	1.92	0.54
423.09408	−0.252	C12H20N6O9S-	5.43E+07	1.67	0.75
423.10532	−0.268	C11H20N8O8S-	4.90E+07	1.82	0.73
423.13041	−0.122	C13H24N6O8S-	8.44E+07	1.85	0.62
423.14164	−0.115	C12H24N8O7S-	5.92E+07	2	0.58
424.08924	−0.041	C11H19N7O9S-	3.86E+07	1.73	0.82
424.11433	0.105	C13H23N5O9S-	5.07E+07	1.77	0.69
424.1256	0.018	C12H23N7O8S-	8.62E+07	1.92	0.67
425.10965	−0.062	C12H22N6O9S-	7.58E+07	1.83	0.75
425.12093	−0.173	C11H22N8O8S-	6.60E+07	2	0.73
425.14597	0.091	C13H26N6O8S-	4.70E+07	2	0.62
426.09372	−0.189	C12H21N5O10S-	3.59E+07	1.75	0.83
426.10497	−0.229	C11H21N7O9S-	6.81E+07	1.91	0.82
426.14125	0.018	C12H25N7O8S-	5.19E+07	2.08	0.67
427.08894	−0.121	C11H20N6O10S-	3.50E+07	1.82	0.91
427.12525	0.055	C12H24N6O9S-	5.92E+07	2	0.75
427.13645	0.132	C11H24N8O8S-	3.55E+07	2.18	0.73
428.12051	0.029	C11H23N7O9S-	5.62E+07	2.09	0.82
429.10454	−0.003	C11H22N6O10S-	4.09E+07	2	0.91
430.11509	−0.11	C14H21N7O7S-	3.49E+07	1.5	0.5
431.1353	0.333	C15H24N6O7S-	4.06E+07	1.6	0.47
432.13068	0.029	C14H23N7O7S-	6.01E+07	1.64	0.5
433.126	−0.135	C13H22N8O7S-	5.78E+07	1.69	0.54
434.11002	−0.144	C13H21N7O8S-	5.78E+07	1.62	0.62
434.14625	0.213	C14H25N7O7S-	7.45E+07	1.79	0.5
435.10529	−0.192	C12H20N8O8S-	4.07E+07	1.67	0.67
435.13033	0.065	C14H24N6O8S-	7.48E+07	1.71	0.57
435.14162	−0.065	C13H24N8O7S-	7.93E+07	1.85	0.54
435.18616	−0.321	C24H28N4O2S-	1.26E+08	1.17	0.08
436.11445	−0.173	C14H23N5O9S-	4.37E+07	1.64	0.64
436.1257	−0.212	C13H23N7O8S-	1.03E+08	1.77	0.62
436.13696	−0.274	C12H23N9O7S-	5.16E+07	1.92	0.58
437.10964	−0.038	C13H22N6O9S-	7.23E+07	1.69	0.69
437.14598	0.065	C14H26N6O8S-	7.46E+07	1.86	0.57
437.15725	−0.019	C13H26N8O7S-	5.83E+07	2	0.54
437.16535	−0.148	C23H26N4O3S-	1.30E+08	1.13	0.13
438.0936	0.09	C13H21N5O10S-	3.29E+07	1.62	0.77
438.10491	−0.086	C12H21N7O9S-	7.11E+07	1.75	0.75
438.11617	−0.147	C11H21N9O8S-	3.59E+07	1.91	0.73
438.13002	0.01	C14H25N5O9S-	5.30E+07	1.79	0.64
438.14129	−0.074	C13H25N7O8S-	1.02E+08	1.92	0.62
439.10005	0.163	C11H20N8O9S-	3.75E+07	1.82	0.82
439.12521	0.145	C13H24N6O9S-	8.54E+07	1.85	0.69
439.13647	0.083	C12H24N8O8S-	8.34E+07	2	0.67
440.10927	0.044	C13H23N5O10S-	4.72E+07	1.77	0.77
440.12052	0.006	C12H23N7O9S-	9.47E+07	1.92	0.75
440.13179	−0.078	C11H23N9O8S-	4.57E+07	2.09	0.73
441.10458	−0.094	C12H22N6O10S-	6.30E+07	1.83	0.83
441.1158	−0.065	C11H22N8O9S-	6.21E+07	2	0.82
441.14089	0.076	C13H26N6O9S-	6.15E+07	2	0.69
442.09979	−0.006	C11H21N7O10S-	4.40E+07	1.91	0.91
442.1362	−0.062	C12H25N7O9S-	6.54E+07	2.08	0.75
443.12007	0.267	C12H24N6O10S-	4.83E+07	2	0.83
444.11547	−0.073	C11H23N7O10S-	3.49E+07	2.09	0.91
446.10996	−0.006	C14H21N7O8S-	3.05E+07	1.5	0.57
447.1303	0.131	C15H24N6O8S-	4.52E+07	1.6	0.53
448.12552	0.195	C14H23N7O8S-	6.81E+07	1.64	0.57
448.1702	−0.365	C25H27N3O3S-	1.04E+08	1.08	0.12
449.10961	0.03	C14H22N6O9S-	3.64E+07	1.57	0.64
449.1209	−0.097	C13H22N8O8S-	6.07E+07	1.69	0.62

Table 3
(Continued)

m/z (exp)	Error (ppm)	Molecular Ion Formula	Intensity/Arbitrary Units	H/C	O/C
449.15711	0.293	C14H26N8O7S-	6.54E+07	1.86	0.5
450.10483	0.094	C13H21N7O9S-	4.38E+07	1.62	0.69
450.14118	0.172	C14H25N7O8S-	9.26E+07	1.79	0.57
450.1494	−0.219	C24H25N3O4S-	6.12E+07	1.04	0.17
450.15257	−0.177	C13H25N9O7S-	5.18E+07	1.92	0.54
451.12529	−0.037	C14H24N6O9S-	6.92E+07	1.71	0.64
451.13654	−0.074	C13H24N8O8S-	9.35E+07	1.85	0.62
452.12046	0.138	C13H23N7O9S-	8.05E+07	1.77	0.69
452.13172	0.079	C12H23N9O8S-	4.96E+07	1.92	0.67
452.1568	0.238	C14H27N7O8S-	6.91E+07	1.93	0.57
452.17628	−0.211	C23H27N5O3S-	7.22E+07	1.17	0.13
453.11585	−0.173	C12H22N8O9S-	6.07E+07	1.83	0.75
453.14098	−0.125	C14H26N6O9S-	6.65E+07	1.86	0.64
453.15224	−0.184	C13H26N8O8S-	7.38E+07	2	0.62
454.09971	0.171	C12H21N7O10S-	3.92E+07	1.75	0.83
454.12486	0.175	C14H25N5O10S-	3.50E+07	1.79	0.71
454.13613	0.094	C13H25N7O9S-	8.16E+07	1.92	0.69
454.14742	−0.032	C12H25N9O8S-	4.54E+07	2.08	0.67
455.12009	0.216	C13H24N6O10S-	5.86E+07	1.85	0.77
455.13134	0.179	C12H24N8O9S-	6.70E+07	2	0.75
456.1154	0.082	C12H23N7O10S-	5.15E+07	1.92	0.83
456.12673	−0.13	C11H23N9O9S-	3.08E+07	2.09	0.82
457.09937	0.183	C12H22N6O11S-	2.29E+07	1.83	0.92
457.11074	−0.117	C11H22N8O10S-	2.79E+07	2	0.91
457.13586	−0.047	C13H26N6O10S-	4.09E+07	2	0.77
461.20179	−0.259	C26H30N4O2S-	8.23E+07	1.15	0.08
462.14121	0.103	C15H25N7O8S-	5.91E+07	1.67	0.53
463.12523	0.094	C15H24N6O9S-	3.85E+07	1.6	0.6
463.13644	0.144	C14H24N8O8S-	6.44E+07	1.71	0.57
463.18105	−0.247	C25H28N4O3S-	9.18E+07	1.12	0.12
464.12047	0.113	C14H23N7O9S-	5.00E+07	1.64	0.64
464.13165	0.227	C13H23N9O8S-	4.24E+07	1.77	0.62
465.11569	0.175	C13H22N8O9S-	4.13E+07	1.69	0.69
465.1521	0.121	C14H26N8O8S-	7.32E+07	1.86	0.57
465.16034	−0.3	C24H26N4O4S-	5.58E+07	1.08	0.17
466.1361	0.156	C14H25N7O9S-	7.79E+07	1.79	0.64
466.14736	0.098	C13H25N9O8S-	6.42E+07	1.92	0.62
467.12011	0.168	C14H24N6O10S-	4.59E+07	1.71	0.71
467.13135	0.153	C13H24N8O9S-	7.36E+07	1.85	0.69
468.11535	0.187	C13H23N7O10S-	5.05E+07	1.77	0.77
468.12662	0.108	C12H23N9O9S-	4.12E+07	1.92	0.75
468.15174	0.176	C14H27N7O9S-	7.40E+07	1.93	0.64
468.16311	−0.116	C13H27N9O8S-	3.96E+07	2.08	0.62
469.13574	0.21	C14H26N6O10S-	5.17E+07	1.86	0.71
469.14703	0.088	C13H26N8O9S-	6.80E+07	2	0.69
470.13106	0.058	C13H25N7O10S-	5.85E+07	1.92	0.77
471.11514	−0.077	C13H24N6O11S-	2.89E+07	1.85	0.85
471.12628	0.12	C12H24N8O10S-	4.11E+07	2	0.83
472.1103	0.111	C12H23N7O11S-	2.20E+07	1.92	0.92
475.12517	0.218	C16H24N6O9S-	2.09E+07	1.5	0.56
477.15208	0.16	C15H26N8O8S-	6.81E+07	1.73	0.53
477.19666	−0.156	C26H30N4O3S-	1.09E+08	1.15	0.12
477.96586	0.039	C10H17N5O7S5-	2.14E+07	1.7	0.7
478.13619	−0.037	C15H25N7O9S-	5.71E+07	1.67	0.6
478.14746	−0.114	C14H25N9O8S-	5.86E+07	1.79	0.57
479.12013	0.122	C15H24N6O10S-	2.86E+07	1.6	0.67
479.13138	0.087	C14H24N8O9S-	5.49E+07	1.71	0.64
479.14271	−0.116	C13H24N10O8S-	2.85E+07	1.85	0.62
479.16771	0.201	C15H28N8O8S-	6.71E+07	1.87	0.53
479.17595	−0.208	C25H28N4O4S-	1.01E+08	1.12	0.16
480.11538	0.12	C14H23N7O10S-	3.60E+07	1.64	0.71
480.12657	0.209	C13H23N9O9S-	3.77E+07	1.77	0.69
480.15172	0.213	C15H27N7O9S-	6.97E+07	1.8	0.6
480.16306	−0.009	C14H27N9O8S-	6.02E+07	1.93	0.57

Table 3
(Continued)

m/z (exp)	Error (ppm)	Molecular Ion Formula	Intensity/Arbitrary Units	H/C	O/C
480.17124	−0.293	C24H27N5O4S-	4.93E+07	1.13	0.17
481.13586	−0.045	C15H26N6O10S-	4.52E+07	1.73	0.67
481.14712	−0.101	C14H26N8O9S-	8.01E+07	1.86	0.64
481.15524	−0.259	C24H26N4O5S-	5.27E+07	1.08	0.21
482.13102	0.14	C14H25N7O10S-	5.88E+07	1.79	0.71
482.1423	0.043	C13H25N9O9S-	5.86E+07	1.92	0.69
482.16736	0.233	C15H29N7O9S-	4.84E+07	1.93	0.6
483.12624	0.2	C13H24N8O10S-	5.07E+07	1.85	0.77
483.16266	0.127	C14H28N8O9S-	5.37E+07	2	0.64
484.1468	−0.129	C14H27N7O10S-	5.68E+07	1.93	0.71
485.14195	0.075	C13H26N8O10S-	4.40E+07	2	0.77
489.15207	0.177	C16H26N8O8S-	4.41E+07	1.63	0.5
490.06689	−0.238	C11H21N7O11S2-	1.67E+07	1.91	1
490.1475	−0.193	C15H25N9O8S-	4.15E+07	1.67	0.53
491.13134	0.166	C15H24N8O9S-	3.14E+07	1.6	0.6
492.15184	−0.036	C16H27N7O9S-	4.79E+07	1.69	0.56
492.16318	−0.253	C15H27N9O8S-	5.70E+07	1.8	0.53
493.14709	−0.038	C15H26N8O9S-	6.05E+07	1.73	0.6
493.15832	−0.031	C14H26N10O8S-	3.61E+07	1.86	0.57
494.13115	−0.126	C15H25N7O10S-	3.85E+07	1.67	0.67
494.1424	−0.161	C14H25N9O9S-	5.05E+07	1.79	0.64
494.16745	0.046	C16H29N7O9S-	5.34E+07	1.81	0.56
494.17878	−0.151	C15H29N9O8S-	4.94E+07	1.93	0.53
495.12636	−0.047	C14H24N8O10S-	3.86E+07	1.71	0.71
495.13769	−0.243	C13H24N10O9S-	2.27E+07	1.85	0.69
495.15138	0.219	C16H28N6O10S-	3.28E+07	1.75	0.63
495.16268	0.084	C15H28N8O9S-	6.64E+07	1.87	0.6
495.17408	−0.253	C14H28N10O8S-	3.27E+07	2	0.57
496.12144	0.293	C13H23N9O10S-	2.10E+07	1.77	0.77
496.15789	0.162	C14H27N9O9S-	5.71E+07	1.93	0.64
496.166	0.029	C24H27N5O5S-	3.60E+07	1.13	0.21
497.14207	−0.168	C14H26N8O10S-	5.32E+07	1.86	0.71
497.15332	−0.202	C13H26N10O9S-	3.61E+07	2	0.69
497.17513	0.106	C26H30N2O6S-	2.17E+08	1.15	0.23
497.1784	−0.057	C15H30N8O9S-	4.19E+07	2	0.6
498.12605	−0.095	C14H25N7O11S-	3.33E+07	1.79	0.79
498.13726	−0.049	C13H25N9O10S-	3.74E+07	1.92	0.77
498.16235	0.075	C15H29N7O10S-	4.63E+07	1.93	0.67
499.12123	0.043	C13H24N8O11S-	2.37E+07	1.85	0.85
499.15753	0.213	C14H28N8O10S-	4.27E+07	2	0.71
503.16775	0.112	C17H28N8O8S-	3.79E+07	1.65	0.47
504.08244	−0.033	C12H23N7O11S2-	1.35E+07	1.92	0.92
504.15172	0.203	C17H27N7O9S-	2.77E+07	1.59	0.53
504.16309	−0.068	C16H27N9O8S-	4.33E+07	1.69	0.5
505.14708	−0.017	C16H26N8O9S-	3.86E+07	1.63	0.56
505.18354	−0.165	C17H30N8O8S-	4.28E+07	1.76	0.47
506.06185	−0.319	C11H21N7O12S2-	1.54E+07	1.91	1.09
506.14243	−0.216	C15H25N9O9S-	3.42E+07	1.67	0.6
506.16742	0.104	C17H29N7O9S-	4.04E+07	1.71	0.53
506.17872	−0.029	C16H29N9O8S-	4.82E+07	1.81	0.5
507.12624	0.19	C15H24N8O10S-	2.52E+07	1.6	0.67
507.13764	−0.139	C14H24N10O9S-	1.74E+07	1.71	0.64
507.16272	0.003	C16H28N8O9S-	5.48E+07	1.75	0.56
507.17412	−0.326	C15H28N10O8S-	4.02E+07	1.87	0.53
507.22453	−0.535	C19H36N6O8S-	3.57E+07	1.89	0.42
508.14673	0.015	C16H27N7O10S-	3.83E+07	1.69	0.63
508.15801	−0.078	C15H27N9O9S-	5.67E+07	1.8	0.6
508.18313	−0.015	C17H31N7O9S-	3.19E+07	1.82	0.53
509.142	−0.027	C15H26N8O10S-	4.37E+07	1.73	0.67
509.15334	−0.237	C14H26N10O9S-	2.95E+07	1.86	0.64
509.17842	−0.095	C16H30N8O9S-	4.67E+07	1.88	0.56
510.12615	−0.289	C15H25N7O11S-	2.08E+07	1.67	0.73
510.13727	−0.068	C14H25N9O10S-	3.18E+07	1.79	0.71
510.1624	−0.025	C16H29N7O10S-	4.24E+07	1.81	0.63

Table 3
(Continued)

m/z (exp)	Error (ppm)	Molecular Ion Formula	Intensity/Arbitrary Units	H/C	O/C
510.17368	−0.117	C15H29N9O9S-	5.25E+07	1.93	0.6
510.18169	−0.05	C25H29N5O5S-	6.94E+07	1.16	0.2
511.15763	0.013	C15H28N8O10S-	5.24E+07	1.87	0.67
511.16565	0.06	C25H28N4O6S-	5.29E+07	1.12	0.24
511.16901	−0.275	C14H28N10O9S-	3.64E+07	2	0.64
512.14177	−0.229	C15H27N7O11S-	3.00E+07	1.8	0.73
512.1529	−0.028	C14H27N9O10S-	4.06E+07	1.93	0.71
518.17871	−0.009	C17H29N9O8S-	3.89E+07	1.71	0.47
519.16272	0.003	C17H28N8O9S-	3.84E+07	1.65	0.53
520.14674	−0.005	C17H27N7O10S-	2.18E+07	1.59	0.59
520.15799	−0.037	C16H27N9O9S-	4.31E+07	1.69	0.56
520.18323	−0.207	C18H31N7O9S-	3.31E+07	1.72	0.5
521.15334	−0.231	C15H26N10O9S-	2.88E+07	1.73	0.6
521.17848	−0.208	C17H30N8O9S-	4.51E+07	1.76	0.53
521.18972	−0.222	C16H30N10O8S-	3.67E+07	1.88	0.5
521.24015	−0.463	C20H38N6O8S-	2.60E+07	1.9	0.4
522.09298	0.016	C12H25N7O12S2-	1.67E+07	2.08	1
522.13732	−0.162	C15H25N9O10S-	2.25E+07	1.67	0.67
522.16234	0.091	C17H29N7O10S-	2.86E+07	1.71	0.59
522.17359	0.058	C16H29N9O9S-	5.59E+07	1.81	0.56
523.12121	0.079	C15H24N8O11S-	1.37E+07	1.6	0.73
523.1576	0.07	C16H28N8O10S-	4.39E+07	1.75	0.63
523.16581	−0.248	C26H28N4O6S-	2.86E+07	1.08	0.23
523.16888	−0.02	C15H28N10O9S-	4.34E+07	1.87	0.6
523.24596	−0.57	C22H36N8O5S-	3.43E+07	1.64	0.23
524.14162	0.062	C16H27N7O11S-	2.38E+07	1.69	0.69
524.15289	−0.009	C15H27N9O10S-	4.07E+07	1.8	0.67
524.17798	0.11	C17H31N7O10S-	3.13E+07	1.82	0.59
524.18931	−0.075	C16H31N9O9S-	3.84E+07	1.94	0.56
524.1973	0.028	C26H31N5O5S-	1.06E+08	1.19	0.19
525.13691	−0.016	C15H26N8O11S-	2.45E+07	1.73	0.73
525.1482	−0.125	C14H26N10O10S-	2.50E+07	1.86	0.71
525.1733	−0.026	C16H30N8O10S-	4.24E+07	1.88	0.63
525.18465	−0.248	C15H30N10O9S-	2.97E+07	2	0.6
525.19263	−0.127	C25H30N6O5S-	4.58E+07	1.2	0.2
526.13215	0.001	C14H25N9O11S-	1.73E+07	1.79	0.79
526.16856	−0.047	C15H29N9O10S-	3.91E+07	1.93	0.67
528.14777	0.058	C14H27N9O11S-	2.18E+07	1.93	0.79
532.15805	−0.149	C17H27N9O9S-	2.17E+07	1.59	0.53
533.17838	−0.016	C18H30N8O9S-	3.09E+07	1.67	0.5
534.17368	−0.111	C17H29N9O9S-	3.57E+07	1.71	0.53
535.15759	0.087	C17H28N8O10S-	3.02E+07	1.65	0.59
535.16886	0.018	C16H28N10O9S-	3.35E+07	1.75	0.56
535.19412	−0.184	C18H32N8O9S-	3.71E+07	1.78	0.5
536.15288	0.01	C16H27N9O10S-	2.98E+07	1.69	0.63
536.16421	−0.171	C15H27N11O9S-	1.75E+07	1.8	0.6
536.17819	−0.284	C18H31N7O10S-	2.42E+07	1.72	0.56
536.18929	−0.036	C17H31N9O9S-	4.50E+07	1.82	0.53
537.14818	−0.085	C15H26N10O10S-	1.66E+07	1.73	0.67
537.17324	0.087	C17H30N8O10S-	3.94E+07	1.76	0.59
537.18455	−0.057	C16H30N10O9S-	3.98E+07	1.88	0.56
538.15722	0.153	C17H29N7O11S-	2.38E+07	1.71	0.65
538.16865	−0.213	C16H29N9O10S-	4.21E+07	1.81	0.63
538.19355	0.255	C18H33N7O10S-	2.22E+07	1.83	0.56
539.15241	0.262	C16H28N8O11S-	2.77E+07	1.75	0.69
539.16383	−0.084	C15H28N10O10S-	2.99E+07	1.87	0.67
540.14785	−0.092	C15H27N9O11S-	2.38E+07	1.8	0.73
540.18419	−0.008	C16H31N9O10S-	3.41E+07	1.94	0.63
540.19221	0.036	C26H31N5O6S-	8.38E+07	1.19	0.23
541.16819	0.021	C16H30N8O11S-	2.96E+07	1.88	0.69
548.1893	−0.054	C18H31N9O9S-	3.52E+07	1.72	0.5
549.17323	0.103	C18H30N8O10S-	2.40E+07	1.67	0.56
549.24631	−0.462	C20H38N8O8S-	3.49E+07	1.9	0.4
550.16859	−0.099	C17H29N9O10S-	3.24E+07	1.71	0.59

Table 3
(Continued)

m/z (exp)	Error (ppm)	Molecular Ion Formula	Intensity/Arbitrary Units	H/C	O/C
550.1935	0.341	C19H33N7O10S-	1.88E+07	1.74	0.53
550.20495	−0.054	C18H33N9O9S-	3.31E+07	1.83	0.5
551.16391	−0.228	C16H28N10O10S-	2.61E+07	1.75	0.63
551.189	−0.115	C18H32N8O10S-	2.71E+07	1.78	0.56
551.20028	−0.2	C17H32N10O9S-	3.03E+07	1.88	0.53
552.1729	0.095	C18H31N7O11S-	1.98E+07	1.72	0.61
552.18421	−0.044	C17H31N9O10S-	3.87E+07	1.82	0.59
553.16815	0.093	C17H30N8O11S-	3.28E+07	1.76	0.65
553.17958	−0.263	C16H30N10O10S-	3.32E+07	1.88	0.63
553.18763	−0.274	C26H30N6O6S-	1.82E+07	1.15	0.23
554.16342	0.055	C16H29N9O11S-	2.63E+07	1.81	0.69
555.15882	−0.217	C15H28N10O11S-	1.73E+07	1.87	0.73
562.20501	−0.159	C19H33N9O9S-	3.35E+07	1.74	0.47
562.26655	−0.165	C22H41N7O8S-	2.48E+07	1.86	0.36
563.18886	0.136	C19H32N8O10S-	2.40E+07	1.68	0.53
563.20021	−0.072	C18H32N10O9S-	3.08E+07	1.78	0.5
563.22525	0.127	C20H36N8O9S-	2.74E+07	1.8	0.45
564.18424	−0.097	C18H31N9O10S-	2.97E+07	1.72	0.56
564.19548	−0.109	C17H31N11O9S-	2.52E+07	1.82	0.53
564.28216	−0.093	C22H43N7O8S-	1.45E+07	1.95	0.36
565.16827	−0.121	C18H30N8O11S-	2.01E+07	1.67	0.61
565.17959	−0.275	C17H30N10O10S-	2.87E+07	1.76	0.59
566.16352	−0.123	C17H29N9O11S-	2.19E+07	1.71	0.65
566.1747	−0.029	C16H29N11O10S-	1.72E+07	1.81	0.63
566.1999	−0.114	C18H33N9O10S-	3.34E+07	1.83	0.56
567.15865	0.087	C16H28N10O11S-	1.82E+07	1.75	0.69
567.18373	0.214	C18H32N8O11S-	2.39E+07	1.78	0.61
567.19521	−0.221	C17H32N10O10S-	3.31E+07	1.88	0.59
568.17906	0.071	C17H31N9O11S-	2.41E+07	1.82	0.65
568.18715	−0.01	C27H31N5O7S-	2.68E+07	1.15	0.26
569.16312	−0.006	C17H30N8O12S-	1.32E+07	1.76	0.71
569.17432	0.052	C16H30N10O11S-	1.89E+07	1.88	0.69
571.23067	−0.461	C22H36N8O8S-	3.42E+07	1.64	0.36
573.24636	−0.529	C22H38N8O8S-	4.13E+07	1.73	0.36
575.26197	−0.458	C22H40N8O8S-	3.87E+07	1.82	0.36
576.18413	0.096	C19H31N9O10S-	2.02E+07	1.63	0.53
576.28214	−0.056	C23H43N7O8S-	1.81E+07	1.87	0.35
577.17939	0.077	C18H30N10O10S-	2.10E+07	1.67	0.56
577.24108	−0.188	C21H38N8O9S-	2.93E+07	1.81	0.43
577.27742	−0.11	C22H42N8O8S-	2.06E+07	1.91	0.36
578.16345	0.001	C18H29N9O11S-	1.52E+07	1.61	0.61
578.17467	0.023	C17H29N11O10S-	1.63E+07	1.71	0.59
578.19989	−0.094	C19H33N9O10S-	2.81E+07	1.74	0.53
578.28785	0.018	C25H41N9O5S-	1.58E+07	1.64	0.2
579.19515	−0.113	C18H32N10O10S-	2.63E+07	1.78	0.56
579.25638	0.417	C21H40N8O9S-	2.51E+07	1.9	0.43
579.28327	−0.277	C24H40N10O5S-	1.74E+07	1.67	0.21
580.1791	0.001	C18H31N9O11S-	2.20E+07	1.72	0.61
580.19055	−0.373	C17H31N11O10S-	2.27E+07	1.82	0.59
580.30347	0.07	C25H43N9O5S-	1.36E+07	1.72	0.2
581.17437	−0.035	C17H30N10O11S-	2.28E+07	1.76	0.65
581.29902	−0.448	C24H42N10O5S-	2.01E+07	1.75	0.21
582.20591	0.126	C17H33N11O10S-	2.10E+07	1.94	0.59
582.21403	−0.004	C27H33N7O6S-	2.74E+07	1.22	0.22
582.24652	−0.222	C23H37N9O7S-	2.68E+07	1.61	0.3
582.28294	−0.283	C24H41N9O6S-	2.70E+07	1.71	0.25
583.19808	−0.063	C27H32N6O7S-	2.54E+07	1.19	0.26
586.24158	−0.468	C22H37N9O8S-	3.99E+07	1.68	0.36
587.26197	−0.449	C23H40N8O8S-	3.65E+07	1.74	0.35
588.25722	−0.45	C22H39N9O8S-	4.19E+07	1.77	0.36
589.24103	−0.099	C22H38N8O9S-	2.92E+07	1.73	0.41
589.2774	−0.074	C23H42N8O8S-	2.72E+07	1.83	0.35
589.28851	0.135	C22H42N10O7S-	2.21E+07	1.91	0.32
590.19993	−0.16	C20H33N9O10S-	2.01E+07	1.65	0.5

Table 3
(Continued)

m/z (exp)	Error (ppm)	Molecular Ion Formula	Intensity/Arbitrary Units	H/C	O/C
590.27281	−0.346	C22H41N9O8S-	3.28E+07	1.86	0.36
591.1952	−0.195	C19H32N10O10S-	2.30E+07	1.68	0.53
591.23156	−0.153	C20H36N10O9S-	2.76E+07	1.8	0.45
591.25644	0.307	C22H40N8O9S-	2.51E+07	1.82	0.41
592.19048	−0.247	C18H31N11O10S-	2.01E+07	1.72	0.56
593.17444	−0.153	C18H30N10O11S-	1.42E+07	1.67	0.61
593.21077	−0.06	C19H34N10O10S-	2.32E+07	1.79	0.53
593.23294	−0.045	C25H46N4O4S4-	2.32E+07	1.84	0.16
594.19487	−0.201	C19H33N9O11S-	1.81E+07	1.74	0.58
594.20618	−0.331	C18H33N11O10S-	2.12E+07	1.83	0.56
595.19014	−0.236	C18H32N10O11S-	2.49E+07	1.78	0.61
595.27826	−0.396	C24H40N10O6S-	2.29E+07	1.67	0.25
596.17386	0.261	C18H31N9O12S-	1.36E+07	1.72	0.67
596.2621	−0.1	C24H39N9O7S-	2.42E+07	1.63	0.29
596.29852	−0.158	C25H43N9O6S-	1.81E+07	1.72	0.24
597.29392	−0.411	C24H42N10O6S-	2.40E+07	1.75	0.25
598.24147	−0.275	C23H37N9O8S-	2.38E+07	1.61	0.35
598.27776	−0.116	C24H41N9O7S-	3.08E+07	1.71	0.29
599.30956	−0.393	C24H44N10O6S-	1.62E+07	1.83	0.25
600.25705	−0.157	C23H39N9O8S-	3.52E+07	1.7	0.35
600.26828	−0.152	C22H39N11O7S-	3.22E+07	1.77	0.32
600.29345	−0.182	C24H43N9O7S-	2.49E+07	1.79	0.29
601.25253	−0.541	C22H38N10O8S-	3.23E+07	1.73	0.36
601.27734	0.027	C24H42N8O8S-	2.88E+07	1.75	0.33
601.2887	−0.184	C23H42N10O7S-	3.21E+07	1.83	0.3
602.23632	−0.165	C22H37N9O9S-	2.44E+07	1.68	0.41
602.27277	−0.273	C23H41N9O8S-	3.27E+07	1.78	0.35
602.28396	−0.202	C22H41N11O7S-	2.50E+07	1.86	0.32
603.25667	−0.08	C23H40N8O9S-	2.91E+07	1.74	0.39
603.26805	−0.324	C22H40N10O8S-	2.99E+07	1.82	0.36
604.25193	−0.098	C22H39N9O9S-	2.85E+07	1.77	0.41
604.28832	−0.107	C23H43N9O8S-	2.44E+07	1.87	0.35
605.23586	0.044	C22H38N8O10S-	1.78E+07	1.73	0.45
605.27207	0.333	C23H42N8O9S-	2.22E+07	1.83	0.39
605.28338	0.206	C22H42N10O8S-	2.23E+07	1.91	0.36
606.20597	0.022	C19H33N11O10S-	1.74E+07	1.74	0.53
606.26736	0.265	C22H41N9O9S-	1.99E+07	1.86	0.41
607.19008	−0.133	C19H32N10O11S-	1.53E+07	1.68	0.58
608.30966	−0.002	C25H43N11O5S-	1.30E+07	1.72	0.2
609.2057	−0.083	C19H34N10O11S-	2.05E+07	1.79	0.58
609.22782	0.014	C25H46N4O5S4-	1.84E+07	1.84	0.2
609.29385	−0.288	C25H42N10O6S-	1.87E+07	1.68	0.24
609.30522	−0.513	C24H42N12O5S-	1.30E+07	1.75	0.21
610.27764	0.083	C25H41N9O7S-	2.38E+07	1.64	0.28
610.28915	−0.371	C24H41N11O6S-	2.06E+07	1.71	0.25
611.27309	−0.246	C24H40N10O7S-	2.62E+07	1.67	0.29
611.3095	−0.287	C25H44N10O6S-	1.59E+07	1.76	0.24
612.2247	−0.176	C28H35N7O7S-	2.87E+07	1.25	0.25
612.25701	−0.089	C24H39N9O8S-	2.45E+07	1.63	0.33
612.29348	−0.228	C25H43N9O7S-	2.29E+07	1.72	0.28
612.30468	−0.174	C24H43N11O6S-	2.15E+07	1.79	0.25
613.28868	−0.148	C24H42N10O7S-	2.93E+07	1.75	0.29
614.27267	−0.105	C24H41N9O8S-	3.19E+07	1.71	0.33
614.30896	0.05	C25H45N9O7S-	1.97E+07	1.8	0.28
615.2681	−0.399	C23H40N10O8S-	3.15E+07	1.74	0.35
615.30438	−0.228	C24H44N10O7S-	2.48E+07	1.83	0.29
616.25194	−0.113	C23H39N9O9S-	2.51E+07	1.7	0.39
616.26333	−0.368	C22H39N11O8S-	2.36E+07	1.77	0.36
616.28832	−0.105	C24H43N9O8S-	2.39E+07	1.79	0.33
616.29951	−0.035	C23H43N11O7S-	1.62E+07	1.87	0.3
617.28353	−0.041	C23H42N10O8S-	3.10E+07	1.83	0.35
618.2675	0.033	C23H41N9O9S-	2.26E+07	1.78	0.39
619.22632	0.104	C21H36N10O10S-	1.69E+07	1.71	0.48
619.26263	0.225	C22H40N10O9S-	2.35E+07	1.82	0.41

Table 3
(Continued)

m/z (exp)	Error (ppm)	Molecular Ion Formula	Intensity/Arbitrary Units	H/C	O/C
620.21037	0.049	C21H35N9O11S-	1.23E+07	1.67	0.52
623.30947	−0.233	C26H44N10O6S-	1.29E+07	1.69	0.23
624.30464	−0.107	C25H43N11O6S-	1.85E+07	1.72	0.24
625.28878	−0.305	C25H42N10O7S-	2.16E+07	1.68	0.28
625.30011	−0.46	C24H42N12O6S-	1.56E+07	1.75	0.25
626.28385	−0.018	C24H41N11O7S-	2.36E+07	1.71	0.29
626.32035	−0.202	C25H45N11O6S-	1.48E+07	1.8	0.24
627.30436	−0.192	C25H44N10O7S-	2.09E+07	1.76	0.28
628.28826	−0.007	C25H43N9O8S-	2.39E+07	1.72	0.32
629.28382	−0.501	C24H42N10O8S-	2.95E+07	1.75	0.33
629.31941	0.017	C25H54N6O6S3-	1.16E+07	2.16	0.24
630.26751	0.017	C24H41N9O9S-	2.14E+07	1.71	0.38
631.29914	0.023	C24H44N10O8S-	2.02E+07	1.83	0.33
632.28288	0.459	C24H43N9O9S-	2.08E+07	1.79	0.38
633.27816	0.41	C23H42N10O9S-	2.28E+07	1.83	0.39
634.22604	0.017	C22H37N9O11S-	1.21E+07	1.68	0.5
637.20066	−0.15	C20H34N10O12S-	1.11E+07	1.7	0.6
638.32049	−0.418	C26H45N11O6S-	1.35E+07	1.73	0.23
639.26774	0.179	C25H40N10O8S-	1.75E+07	1.6	0.32
639.30422	0.031	C26H44N10O7S-	1.60E+07	1.69	0.27
639.31559	−0.184	C25H44N12O6S-	1.51E+07	1.76	0.24
640.29956	−0.112	C25H43N11O7S-	2.02E+07	1.72	0.28
641.28364	−0.211	C25H42N10O8S-	2.06E+07	1.68	0.32
641.29491	−0.269	C24H42N12O7S-	2.10E+07	1.75	0.29
641.31984	0.077	C26H46N10O7S-	1.54E+07	1.77	0.27
642.26732	0.312	C25H41N9O9S-	1.82E+07	1.64	0.36
642.30399	−0.132	C26H45N9O8S-	1.67E+07	1.73	0.31
642.31512	0.029	C25H45N11O7S-	1.70E+07	1.8	0.28
643.29901	0.225	C25H44N10O8S-	1.91E+07	1.76	0.32
644.25802	−0.002	C23H39N11O9S-	1.66E+07	1.7	0.39
644.28285	0.497	C25H43N9O9S-	2.01E+07	1.72	0.36
644.29435	0.083	C24H43N11O8S-	2.55E+07	1.79	0.33
645.27818	0.371	C24H42N10O9S-	2.09E+07	1.75	0.38
645.31469	0.177	C25H46N10O8S-	1.24E+07	1.84	0.32
650.23971	−0.182	C23H41N9O9S2-	1.53E+07	1.78	0.39
651.2163	−0.131	C21H36N10O12S-	1.07E+07	1.71	0.57
654.27895	−0.3	C25H41N11O8S-	1.69E+07	1.64	0.32
654.31513	0.013	C26H45N11O7S-	1.67E+07	1.73	0.27
655.26251	0.396	C25H40N10O9S-	1.34E+07	1.6	0.36
655.29903	0.19	C26H44N10O8S-	1.37E+07	1.69	0.31
656.29436	0.066	C25H43N11O8S-	1.91E+07	1.72	0.32
656.33077	0.028	C26H47N11O7S-	1.11E+07	1.81	0.27
657.27837	0.075	C25H42N10O9S-	1.58E+07	1.68	0.36
657.32621	−0.262	C25H46N12O7S-	1.04E+07	1.84	0.28
658.31006	−0.01	C25H45N11O8S-	1.54E+07	1.8	0.32
659.29376	0.469	C25H44N10O9S-	1.83E+07	1.76	0.36
660.25305	−0.176	C23H39N11O10S-	1.32E+07	1.7	0.43
660.27781	0.417	C25H43N9O10S-	1.43E+07	1.72	0.4
661.27324	0.143	C24H42N10O10S-	1.64E+07	1.75	0.42
661.30944	0.423	C25H46N10O9S-	1.37E+07	1.84	0.36
661.33462	0.38	C27H50N8O9S-	7.36E+06	1.85	0.33
665.24012	0.007	C25H46N8O5S4-	1.40E+07	1.84	0.2
665.25083	0.468	C31H38N8O7S-	1.27E+07	1.23	0.23
667.21126	−0.196	C21H36N10O13S-	8.07E+06	1.71	0.62
667.31039	−0.004	C26H44N12O7S-	1.45E+07	1.69	0.27
668.29431	0.14	C26H43N11O8S-	1.31E+07	1.65	0.31
668.33072	0.102	C27H47N11O7S-	9.03E+06	1.74	0.26
669.28975	−0.146	C25H42N12O8S-	1.53E+07	1.68	0.32
669.32615	−0.168	C26H46N12O7S-	1.30E+07	1.77	0.27
671.29397	0.148	C26H44N10O9S-	1.42E+07	1.69	0.35
671.3054	−0.145	C25H44N12O8S-	1.48E+07	1.76	0.32
671.3305	−0.068	C27H48N10O8S-	1.02E+07	1.78	0.3
672.28897	0.518	C25H43N11O9S-	1.89E+07	1.72	0.36
672.32562	0.124	C26H47N11O8S-	1.30E+07	1.81	0.31

Table 3
(Continued)

m/z (exp)	Error (ppm)	Molecular Ion Formula	Intensity/Arbitrary Units	H/C	O/C
673.30956	0.237	C26H46N10O9S-	1.13E+07	1.77	0.35
673.32091	0.063	C25H46N12O8S-	1.03E+07	1.84	0.32
675.32514	0.34	C26H48N10O9S-	1.00E+07	1.85	0.35
677.25057	−0.117	C24H42N10O9S2-	1.04E+07	1.75	0.38
677.28642	−0.02	C25H54N6O7S4-	1.98E+07	2.16	0.28
677.34089	0.191	C26H50N10O9S-	8.69E+06	1.92	0.35
678.25202	0.362	C24H41N9O12S-	8.31E+06	1.71	0.5
684.3369	0.053	C26H47N13O7S-	7.44E+06	1.81	0.27
686.27982	−0.005	C24H41N13O9S-	1.14E+07	1.71	0.38
687.3004	−0.266	C25H44N12O9S-	1.12E+07	1.76	0.36
689.3408	0.318	C27H50N10O9S-	9.97E+06	1.85	0.33
695.27584	0.002	C28H52N6O6S4-	1.10E+07	1.86	0.21
696.33685	0.124	C27H47N13O7S-	8.82E+06	1.74	0.26
698.31603	0.246	C26H45N13O8S-	1.23E+07	1.73	0.31
700.10011	−0.128	C18H31N13O7S5-	1.59E+07	1.72	0.39
700.32027	0.498	C27H47N11O9S-	1.07E+07	1.74	0.33
700.33181	0.059	C26H47N13O8S-	1.12E+07	1.81	0.31
701.28638	0.038	C27H54N6O7S4-	1.80E+07	2	0.26
701.31602	−0.217	C26H46N12O9S-	9.93E+06	1.77	0.35
703.32037	−0.122	C27H48N10O10S-	7.54E+06	1.78	0.37
706.27694	0.141	C25H45N11O9S2-	9.58E+06	1.8	0.36
709.29414	0.457	C25H46N10O12S-	8.63E+06	1.84	0.48
713.35209	0.228	C28H50N12O8S-	5.54E+06	1.79	0.29
718.277	0.055	C26H45N11O9S2-	8.97E+06	1.73	0.35
721.2942	0.367	C26H46N10O12S-	7.26E+06	1.77	0.46
722.26451	0.071	C23H41N13O12S-	5.65E+06	1.78	0.52
726.34744	0.085	C28H49N13O8S-	6.42E+06	1.75	0.29
728.36306	0.126	C28H51N13O8S-	6.27E+06	1.82	0.29
730.37874	0.084	C28H53N13O8S-	5.95E+06	1.89	0.29
741.28393	0.492	C25H46N10O14S-	6.17E+06	1.84	0.56
742.3788	0.002	C29H53N13O8S-	8.67E+06	1.83	0.28
745.25152	0.045	C26H42N12O10S2-	5.37E+06	1.62	0.38
746.28337	−0.245	C26H45N13O9S2-	6.19E+06	1.73	0.35
753.19854	−0.09	C22H38N14O10S3-	5.75E+06	1.73	0.45
793.13914	0.36	C31H38N8O7S5-	5.38E+06	1.23	0.23
818.30459	−0.333	C29H49N13O11S2-	5.84E+06	1.69	0.38
895.16491	−0.556	C26H40N16O10S5-	6.29E+06	1.54	0.38

Note. The measured, experimental m/z values, its error in ppm (difference between experimental and theoretical m/z values), the assigned molecular ion formula, mass spectrometric intensity, and atomic ratios H/C and O/C are reported.

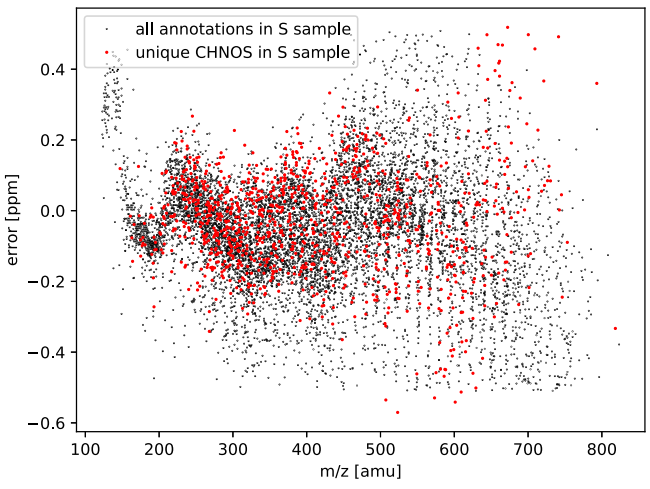

Figure 8. Error plot of formula assignment. 50.1% of all formulas have an error of ±0.1 ppm, 78.5% of all formulas have an error of ±0.2 ppm, and 100% of formula assignments are within ±0.5 ppm.

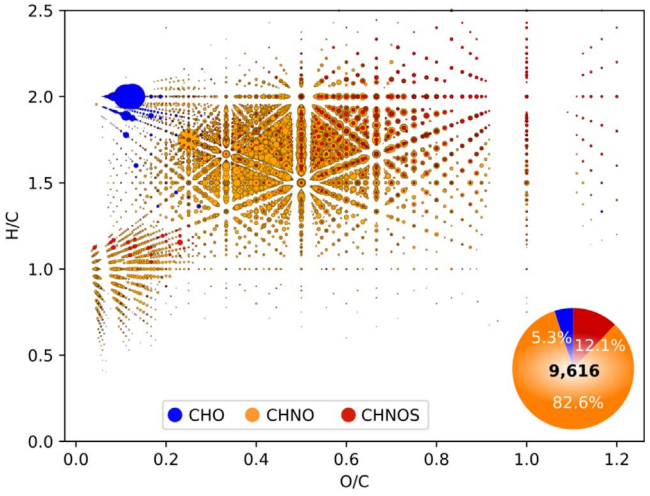

Figure 9. van Krevelen diagram of all annotation including CHO, CHNO, and CHNOS. 12.1% of all assigned molecular formulas bear sulfur, even though the major chemical class consists of CHNO compounds. The bubble size scales with mass spectrometric intensity.

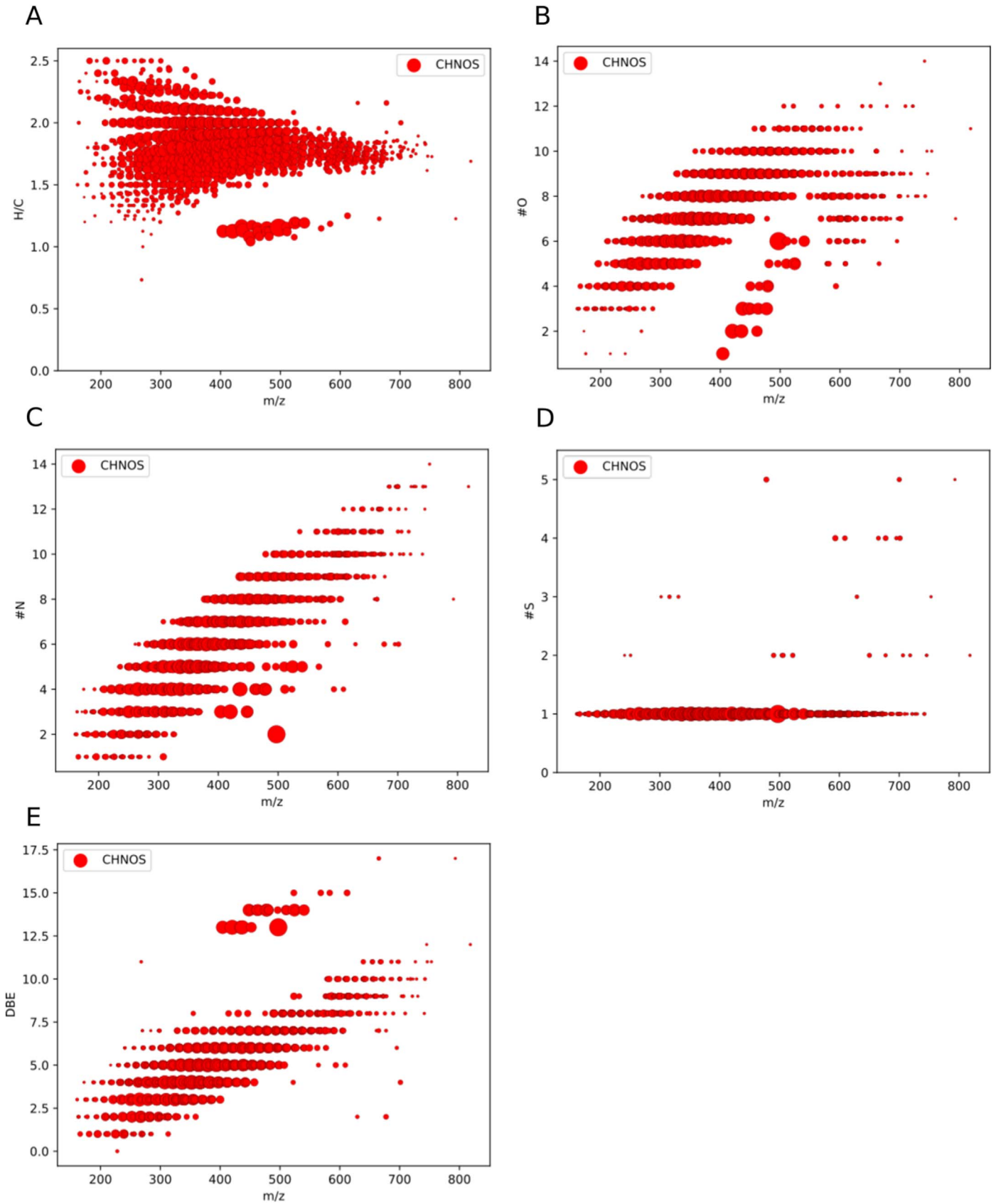

Figure 10. m/z-related representations. (A) H/C vs. m/z plot shows the presence of complete homologues organosulfur series at a fairly high degree of saturation. (B, C, E) Oxygen, nitrogen counts as well as DBE are proportional to molecular mass. (D) #S vs. m/z representation highlight that most detected organosulfur (CHNOS) compounds bear one sulfur atom. The bubble size scales with mass spectrometric intensity.

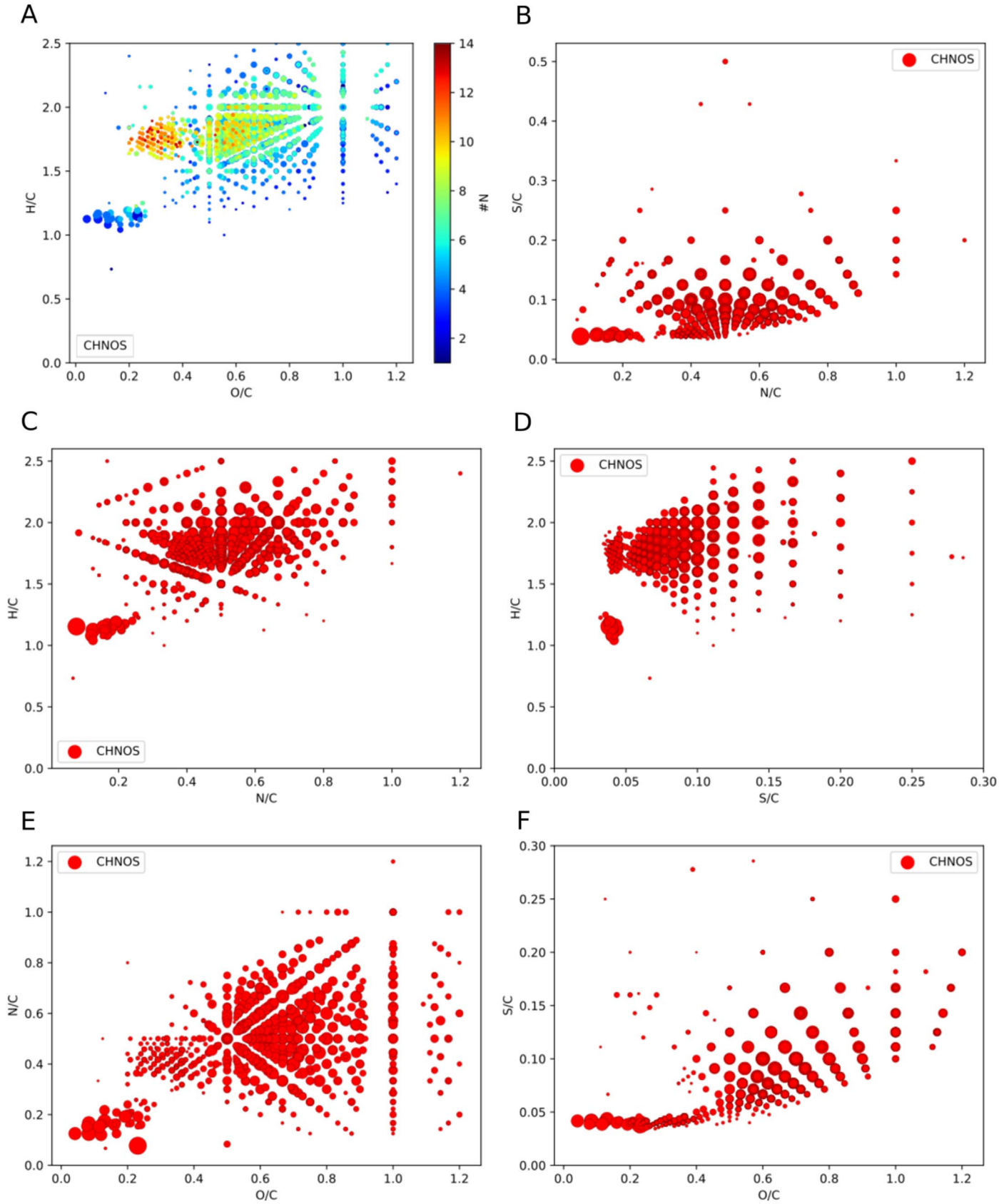

Figure 11. Atomic ratio plots. (A) van Krevelen diagram (H/C vs. O/C) with a nitrogen count color code indicates the presence of different groups within all detected organosulfur compounds. (B,F) S/C vs. N/C and S/C vs. O/C underlines a small sulfur to carbon backbone ratio along a diversity of heteroatoms (N or O). (C, D) H/C vs. N/C and H/C vs. S/C reveal saturated characteristics of organosulfur compounds. (E) N/C vs. O/C plot shows a rich diversity in heteroatom chemistry within the observed organosulfur compounds. The bubble size scales with mass spectrometric intensity.

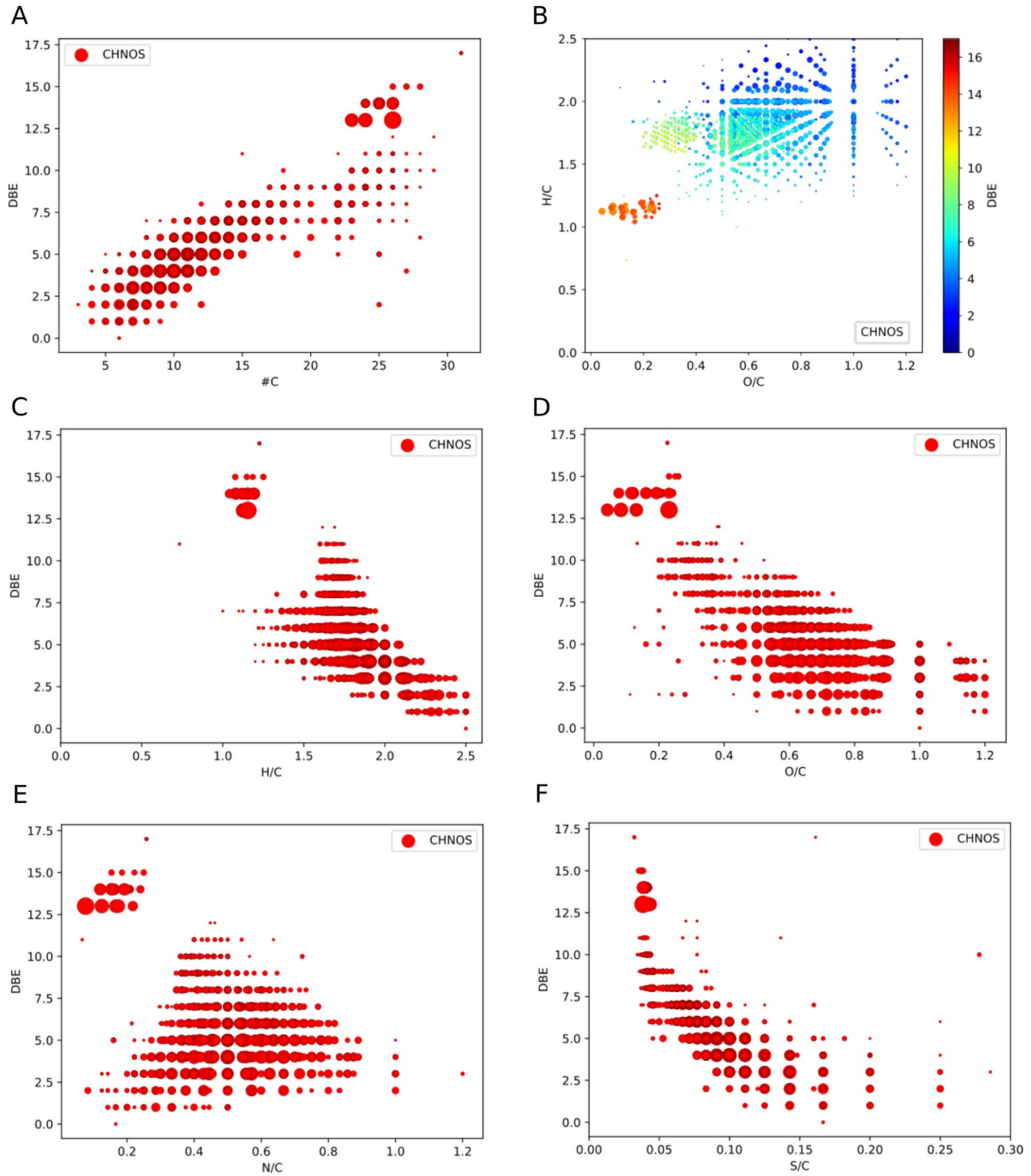

Figure 12. DBE-related representations. (A) DBE scales with carbon counts and is inversely related to H/C (C), O/C (D), N/C (E), and S/C (F). (B) H/C vs. O/C with DBE color code give further evidence for an inverse trend of DBE with both H/C and O/C. The bubble size scales with mass spectrometric intensity.

the significance of the number of sulfur-bearing compounds in the S^{7+}-bombarded astrophysical ice analogs (Figure 9). Due to the complexity and high dimensionality of the obtained FT-ICR-MS data, various types of representations are reported to get as much information as possible. The figures are grouped into four categories, (i) *m-z*-related representations (Figure 10) and (ii) atomic ratio plots (Figure 11), (iii) DBE-related representations (Figure 12), and (iv) atom count distributions (Figure 13).

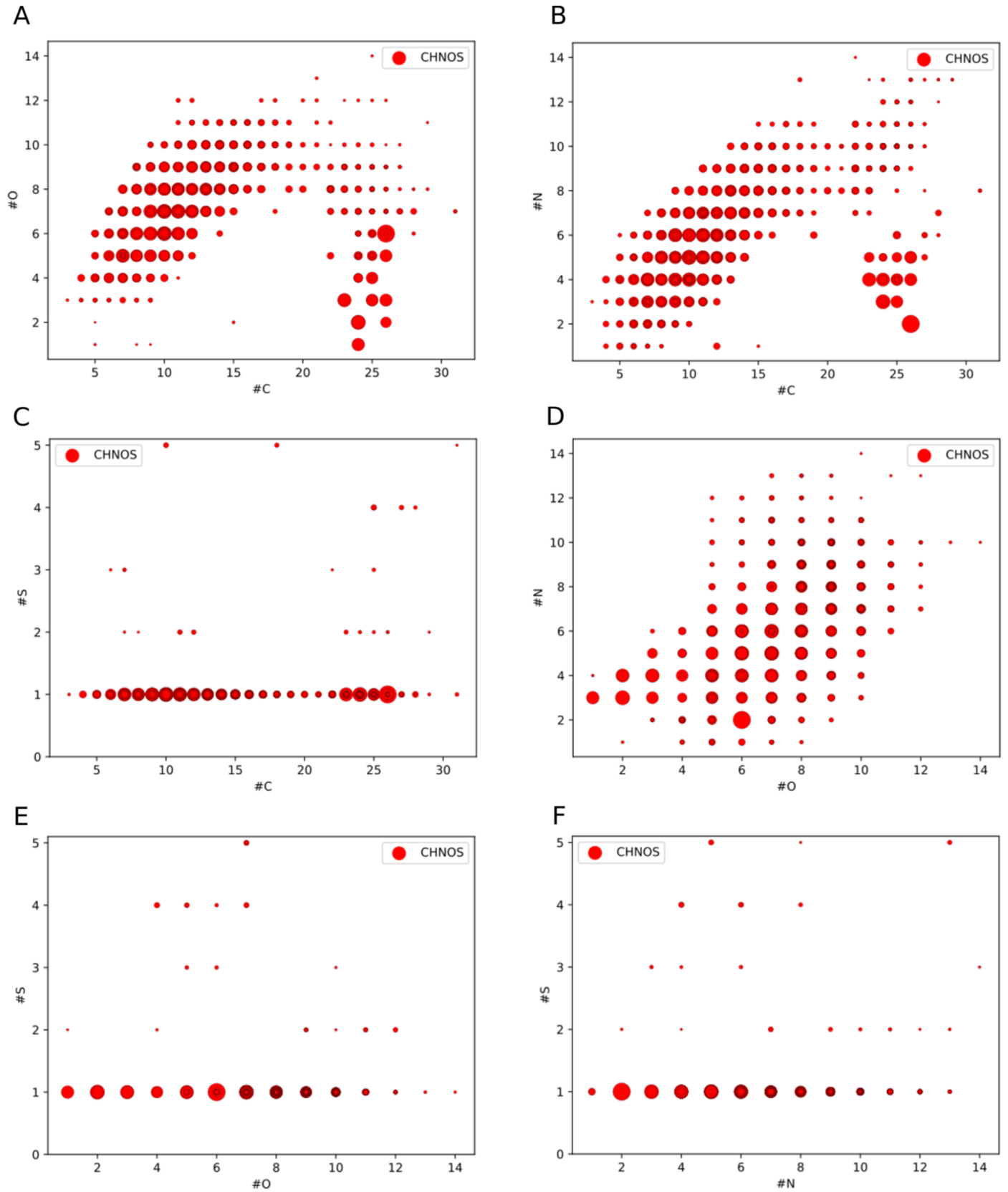

Figure 13. Atom count distributions. (A, B) Oxygen and nitrogen counts vs. carbon counts reveal two separate groups within the observed organosulfur compounds. (C, E, F) Organosulfur compounds bear mostly one sulfur atom. Among these one-S-bearing compounds, different intensity patterns are observed. (D) Nitrogen counts vs. oxygen counts show a large coverage among a large range of heteroatom counts. This indicates a rich diversity in heteroatom chemistry within the observed organosulfur compounds. The bubble size scales with mass spectrometric intensity.

ORCID iDs

Vassilissa Vinogradoff https://orcid.org/0000-0003-4107-0980

References

Altwegg, K., Balsiger, H., Bar-Nun, A., et al. 2015, Sci, 347, 1261952
Altwegg, K., Balsiger, H., Berthelier, J.-J., et al. 2017, MNRAS, 469, S130
Anders, C., & Urbassek, H. M. 2018, MNRAS, 482, 2374
Anders, C., & Urbassek, H. M. 2019, A&A, 625, A140
Augé, B., Been, T., Boduch, P., et al. 2018, RScI, 89, 075105
Barucci, M., Merlin, F., Guilbert, A., et al. 2008, A&A, 479, L13
Bischoff, A., Barrat, J.-A., Berndt, J., et al. 2019, Geoch, in press (doi:10.1016/j.chemer.2019.07.007)
Bisschop, S., Fuchs, G., Boogert, A., Van Dishoeck, E., & Linnartz, H. 2007, A&A, 470, 749
Bockelée-Morvan, D., Crovisier, J., Mumma, M., & Weaver, H. 2004, in Comets II, ed. C. Festou, H. U. Keller, & H. A. Weaver (Tucson, AZ: Univ. Arizona Press), 391
Boduch, P., Brunetto, R., Ding, J., et al. 2016, Icar, 277, 424
Bossa, J., Theule, P., Duvernay, F., & Chiavassa, T. 2009, ApJ, 707, 1524
Brown, M. E., & Calvin, W. M. 2000, Sci, 287, 107
Butscher, T., Duvernay, F., Rimola, A., Segado-Centellas, M., & Chiavassa, T. 2017, PCCP, 19, 2857
Calmonte, U., Altwegg, K., Balsiger, H., et al. 2016, MNRAS, 462, S253
Carlson, R., Anderson, M., Johnson, R., Schulman, M., & Yavrouian, A. 2002, Icar, 157, 456
Carlson, R., Calvin, W., Dalton, J., et al. 2009, in Europa, ed. R. T. Pappalardo, W. B. McKinnon, & K. K. Khurana (Tucson, AZ: Univ. Arizona Press), 283
Chen, Y.-J., Juang, K.-J., Nuevo, M., et al. 2014, ApJ, 798, 80
Colthup, N. 1950, JOSA, 40, 397
Cook, J. C., Desch, S. J., Roush, T. L., Trujillo, C. A., & Geballe, T. 2007, ApJ, 663, 1406
Cooper, J. F., Christian, E. R., Richardson, J. D., & Wang, C. 2004, The First Decadal Review of the Edgeworth-Kuiper Belt (Berlin: Springer), 261
Dalton, J., Cassidy, T., Paranicas, C., et al. 2013, P&SS, 77, 45
Danger, G., Fresneau, A., Mrad, N. A., et al. 2016, GeCoA, 189, 184
Danger, G., Orthous-Daunay, F.-R., de Marcellus, P., et al. 2013, GeCoA, 118, 184
de Marcellus, P., Meinert, C., Myrgorodska, I., et al. 2015, PNAS, 112, 965
De Sanctis, M., Ammannito, E., Raponi, A., et al. 2015, Natur, 528, 241
Desch, S. J., Cook, J. C., Doggett, T., & Porter, S. B. 2009, Icar, 202, 694
Ding, J., Boduch, P., Domaracka, A., et al. 2013, Icar, 226, 860
Ferrante, R. F., Moore, M. H., Spiliotis, M. M., & Hudson, R. L. 2008, ApJ, 684, 1210
Fresneau, A., Mrad, N. A., d'Hendecourt, L. L., et al. 2017, ApJ, 837, 168
Garozzo, M., Fulvio, D., Kanuchova, Z., Palumbo, M., & Strazzulla, G. 2010, A&A, 509, A67
Gerakines, P., Schutte, W., & Ehrenfreund, P. 1996, A&A, 312, 289
Gerakines, P. A., Schutte, W., Greenberg, J., & van Dishoeck, E. F. 1994, arXiv:astro-ph/9409076
Grundy, W., Binzel, R., Buratti, B., et al. 2016, Sci, 351, aad9189
Herbst, E., & Van Dishoeck, E. F. 2009, ARA&A, 47, 427
Hodyss, R., Parkinson, C. D., Johnson, P. V., et al. 2009, GeoRL, 36, L17103
Hudson, R., Moore, M., & Gerakines, P. 2001, ApJ, 550, 1140
Hudson, R. L., Moore, M. H., & Cook, A. M. 2005, AdSpR, 36, 184
Jewitt, D. C., & Luu, J. 2004, Natur, 432, 731
Jiménez-Escobar, A., & Caro, G. M. 2011, A&A, 536, A91
Kerkhof, O., Schutte, W., Ehrenfreund, P., et al. 1999, A&A, 346, 990
Kim, S., Kramer, R. W., & Hatcher, P. G. 2003, AnaCh, 75, 5336
Laas, J. C., & Caselli, P. 2019, A&A, 624, A108
Le Gal, R., Öberg, K. I., Loomis, R. A., Pegues, J., & Bergner, J. B. 2019, ApJ, 876, 72
Loeffler, M., Hudson, R., Moore, M., & Carlson, R. 2011, Icar, 215, 370
Lv, X., Boduch, P., Ding, J., et al. 2013, MNRAS, 438, 922
Lv, X., de Barros, A., Boduch, P., et al. 2012, A&A, 546, A81
Mahjoub, A., Poston, M. J., Blacksberg, J., et al. 2017, ApJ, 846, 148
Maity, S., & Kaiser, R. I. 2013, ApJ, 773, 184
Maki, A. G., & Blaine, L. 1964, JMoSp, 12, 45
Mauk, B., Mitchell, D., McEntire, R., et al. 2004, JGRA, 109
Meinert, C., Myrgorodska, I., De Marcellus, P., et al. 2016, Sci, 352, 208
Moore, M., Hudson, R., & Carlson, R. 2007, Icar, 189, 409
Moore, M. H. 1984, Icar, 59, 114
Mueller, D., Swordy, S. P., Meyer, P., L'Heureux, J., & Grunsfeld, J. M. 1991, ApJ, 374, 356
Muñoz Caro, G., & Schutte, W. 2003, A&A, 412, 121
Neufeld, D., Godard, B., Gerin, M., et al. 2015, A&A, 577, A49
Öberg, K. I. 2016, ChRv, 116, 9631
Palumbo, M., Geballe, T., & Tielens, A. G. 1997, ApJ, 479, 839
Paranicas, C., Cooper, J., Garrett, H., Johnson, R., & Sturner, S. 2009, in Europa, ed. R. T. Pappalardo, W. B. McKinnon, & K. K. Khurana (Tucson, AZ: Univ. Arizona Press), 529
Penzias, A., Solomon, P., Wilson, R., & Jefferts, K. 1971, ApJL, 168, L53
Poston, M. J., Mahjoub, A., Ehlmann, B. L., et al. 2018, ApJ, 856, 124
Prasad, S. S., & Huntress, W. T., Jr. 1982, ApJ, 260, 590
Raunier, S., Chiavassa, T., Marinelli, F., Allouche, A., & Aycard, J. 2003, CPL, 368, 594
Ross, M. N., & Schubert, G. 1990, GeoRL, 17, 1749
Ruf, A., d'Hendecourt, L., & Schmitt-Kopplin, P. 2018, Life, 8, 18
Ruf, A., Kanawati, B., Hertkorn, N., et al. 2017, PNAS, 114, 2819
Ruf, A., Poinot, P., Geffroy, C., Le Sergeant d'Hendecourt, L., & Danger, G. 2019, Life, 9, 35
Schlemmer, S., Giesen, T., Jäger, C., & Mutschke, H. 2015, Laboratory Astrochemistry: from Molecules through Nanoparticles to Grains (New York: Wiley)
Schmitt-Kopplin, P., Gabelica, Z., Gougeon, R. D., et al. 2010, PNAS, 107, 2763
Schmitt-Kopplin, P., Hemmler, D., Moritz, F., et al. 2019, FaDi, 218, 9
Schutte, W., Allamandola, L., & Sandford, S. 1993, Icar, 104, 118
Schutte, W., Boogert, A., Tielens, A., et al. 1999, A&A, 343, 966
Semenov, D., Favre, C., Fedele, D., et al. 2018, A&A, 617, A28
Senior, J. K. 1951, AmJM, 73, 663
Signorell, R., Jetzki, M., Kunzmann, M., & Ueberschaer, R. 2006, JPCA, 110, 2890
Sofia, U. J., Cardelli, J. A., & Savage, B. D. 1994, ApJ, 430, 650
Spencer, J. R., Tamppari, L. K., Martin, T. Z., & Travis, L. D. 1999, Sci, 284, 1514
Strazzulla, G., Baratta, G., Leto, G., & Gomis, O. 2007, Icar, 192, 623
Strazzulla, G., Garozzo, M., & Gomis, O. 2009, AdSpR, 43, 1442
Takashima, T., Doke, T., Hayashi, T., et al. 1997, ApJL, 477, L111
Theulé, P., Duvernay, F., Danger, G., et al. 2013, AdSpR, 52, 1567
Tziotis, D., Hertkorn, N., & Schmitt-Kopplin, P. 2011, Eur. J. Mass Spectrom., 17, 415
Van Dishoeck, E. F. 2014, FaDi, 168, 9
Van Krevelen, D. 1950, Fuel, 29, 269
Van Steenberg, M. E., & Shull, J. M. 1988, ApJ, 330, 942
Vastel, C., Quénard, D., Le Gal, R., et al. 2018, MNRAS, 478, 5514
Von Steiger, R., Schwadron, N., Fisk, L., et al. 2000, JGRA, 105, 27217
von Steiger, R., Zurbuchen, T. H., & McComas, D. J. 2010, GeoRL, 37, L22101
Waite, J. H., Glein, C. R., Perryman, R. S., et al. 2017, Sci, 356, 155
Wu, Z., Rodgers, R. P., & Marshall, A. G. 2004, AnaCh, 76, 2511
Ziegler, J. F., Ziegler, M. D., & Biersack, J. P. 2010, NIMPB, 268, 1818